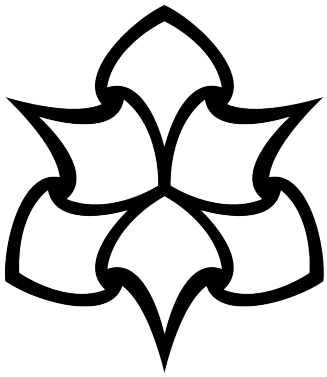

The preparation, characterization and separation of isomeric methylmethcathinone(s) from their reduced methylephedrine counterparts using Hydrophilic Interaction LIquid Chromatography (HILIC).

C P Turnbull

MSc (by Research) 2017

The preparation, characterization and separation of isomeric methylmethcathinone(s) from their reduced methylephedrine counterparts using Hydrophilic Interaction LIquid Chromatography (HILIC).

Christopher Philip Turnbull

Master in Science (by Research)

A thesis submitted in fulfilment of the requirements of the Manchester Metropolitan University for the degree of Master of Science (by Research)

The School of Science & the Environment

Manchester Metropolitan University

Acknowledgements

I would like to thank my supervisors, Dr. Oliver Sutcliffe and Dr. Ryan Mewis, for guiding me through the last two years, as well as the technical staff at MMU for providing support.

I would also like to take the time to thank my family and friends, who have also supported me through the research and the production of this thesis.

Contents

1. List of Figures

2. List of Tables

3. List of Equations

4. Abbreviations

Accident and Emergency	(A&E)
Advisory Council on the Misuse of Drugs	(ACMD)
Aromatic	(Ar)
Capacity factor	(k')
Centre for Drug Evaluation and Research	(CDER)
Correlation SpectroscopY	(COSY)
Dead volume	(t_0)
Dichloromethane	(DCM)
Dimethyl sulfoxide	(DMSO)
ElectroSpray Ionisation	(ESI)
Flow Rate	(FR)
Fourier Transform Infra-Red Spectroscopy-Attenuated Total Reflectance	(FTIR-ATR)
4-Fluoromethcathinone	(4-FMC)
Gas Chromatography – Mass Spectrometery	(GC-MS)
Height Equivalent Theoretical Plates	(HETP)
Heteronuclear Multiple Quantum Coherence	(HMQC)

Heteronuclear Multiple-Quantum Correlation	(HMQC)
High Performance Liquid Chromatography	(HPLC)
Hydrophilic Interaction Liquid Chromatography	(HILIC)
International Council for Harmonisation	(ICH)
Ionic Exchange	(IE)
Ion chromatography	(IC)
Limit of Detection	(LOD)
Limit of Quantification	(LOQ)
Liquid Chromatography Mass Spectroscopy	(LCMS)
Mass Spectrometry/Mass Spectrometry	(MS/MS)
Mass to charge ratio	(m/z)
Methylmethcathinone	(MMC)
2-Methylmethcathinone	(2-MMC)
3-Methylmethcathinone	(3-MMC)
4-Methylmethcathinone	(4-MMC)
New Psychoactive Substances	(NPS)
Nuclear Overhauser Effect	(NOE)
Nuclear Overhauser Effect SpectroscopY	(NOESY)

Number of plates	(N)
Office of National Statistics	(ONS)
Percentage Relative Standard Deviation	(%RSD)
Plate height	(H)
Regression Co-effiecient	(R^2)
Relative Retention Time	(RRT)
Resolution	(R_s)
Retention Time	(t_R)
Reverse Phase	(RP)
Solid Phase Extraction	(SPE)
Temporary Drug Control Orders	(TDCO)
Ultra-Violet and Visible Spectroscopy	(UV-VIS)
United Kingdom	(UK)
United Nations	(UN)
United Nations Office on Drugs and Crime	(UNODC)
United Nations Office on Drugs and Crime Early Warning Advisory on New Psychoactive Substances	(UNODCEWA)

5. Abstract

This thesis is concerned with the synthesis and characterisation of the *ortho*-, *meta*- and *para*-regioisomers of methylephedrine prepared from their corresponding regioisomeric methylmethcathiones. The method principally reduced the carbonyl group (of the cathinone) to a secondary alcohol using sodium borohydride. Crystallisation of the target molecules as their corresponding hydrochloride salts was accomplished using HCl in dioxane (55 – 67% yield). Structural characterisation of the each individual regioisomer was accomplished using a variety of techniques including Nuclear Magnetic Resonance (NMR), Mass Spectrometry (MS), Fourier Transform Infrared Attenuated Total Reflectance (FTIR-ATR), and Ultra Violet – Visible Spectroscopy UV-VIS.

High Performance Liquid Chromatography (HPLC) was used to separate each individual regioisomer around the aromatic ring. This was achieved by Hydrophilic Interaction Liquid Chromatography (HILIC) with Hichrom ACE 5 SIL column and a mobile phase consisting of acetonitrile and aqueous ammonium formate [90:10% v/v]. This method showed a range of Limit of Detection (LOD) values over the three isomers from 0.05 - 0.07 μg mL^{-1} for methylmethcathinone and 0.09 - 0.28 μg mL^{-1} for methylephedrine. A range was also observed for the Limit of Quantification (LOQ) for these compounds, which was 0.15 - 0.22 μg mL^{-1} and 0.28 -0.83 μg mL^{-1} respectively. The method displayed robustness in terms of the mobile phase composition, flow rate and temperature and, following testing with street samples, could be applied to real world applications.

6. Introduction

6.1. Misuse Of Drugs Act 1971

The Act is the result of the United Nations (UN) 1961 convention on narcotic drugs and fulfils the commitment of this convention by segregating controlled substances into three classes: A, B and C.[4-6] The seriousness of the drug in question determines which class it is allocated to, with the most dangerous in A and the least in C, though the Act does have flexibility which allows these controlled substances to be used in certain activities without breaking the law e.g. research projects. However, it cannot keep up with the fast-paced nature of the New/Novel Psychoactive Substance (NPS) market.[7]

Legislation has broken down the punishments of each class with the most severe response being for the class A compounds and the least for the class C. Table 1 breaks down the offences under the Act but also the punitive measures associated with each class and offence.

Table 1 The current punishments for the types of drug crime according to the misuse of the Drugs Act 1971.[8]

Offence	Maximum Penalty for Class A (length in prison)	Maximum Penalty for Class B (length in prison)	Maximum Penalty for Class C (length in prison)
Production	Up to life in prison, an unlimited fine or both	Up to 14 years in prison, an unlimited fine or both	Up to 14 years in prison, an unlimited fine or both
Supply	Up to life in prison, an unlimited fine or both	Up to 14 years in prison, an unlimited fine or both	Up to 14 years in prison, an unlimited fine or both
Possession	Up to 7 years in prison, an unlimited fine or both	Up to 5 years in prison, an unlimited fine or both	Up to 2 years in prison, an unlimited fine or both (except anabolic steroids for personal use)
Possession with intent to supply	Up to life in prison, an unlimited fine or both	Up to 14 years in prison, an unlimited fine or both	Up to 14 years in prison, an unlimited fine or both
Allowing the activities above to take place on premises	14 Years	14 Years	14 Years

This Act has been in place for 37 years and in that time the recreational drug market has changed drastically.[8] The Act has undergone significant alterations since 1971, the biggest being the 2011 Police and Social Reforms Act which created Temporary Drug Control Orders (TDCO).[5, 7, 9] With TDCOs, the government can add new drugs to the list without the lengthy process of going through Parliament, however, these orders are only valid for a period of 12 months.[5, 7, 8] Anyone caught with a drug on a TDCO will not be arrested for possession, however, the police can seize any material they believe to be on a TCDO. The reason for this short time is to allow the Advisory Council on the Misuse of Drugs (ACMD) [5, 7, 8] to review the new drug and assess whether amendments to the Misuse of Drugs Act is required. These TCDOs were a stopgap in the fight against dangerous drugs being supplied on the street, but the change in the market has been too quick, vast and unpredictable that minor

changes in legislature have proved inadequate to keep up. A change in stance from the U.K. government was required to implement a new Act dealing with the fresh developments in the drug markets, specifically the Psychoactive Substances Act 2016 (PSA 2016).[7]

6.2. Psychoactive Substances Act 2016

Introduction of the PSA 2016 means that any chemical that has an ability to create a psychoactive effect in a human being is illegal to supply, or possess with the intent to supply, and carries a maximum sentence of 7 years.[7] The Act does not say that it is illegal to possess. This legislation has resulted in heated discourse, with claims it will be scientifically and therefore legally unenforceable.[7] Determining whether a substance is "psychoactive" is a difficult and complex process as the effects, whether harmful or not, are unable to be substantiated unless human trials are conducted e.g. to determine the true addictiveness of the new drug.[7] It is possible to conduct the trials *in vitro.* Although this test is less controversial and costly than human trials, it is yet to be fully developed into a consistent and reliable framework.[10] The Act states that a compound is a NPS if it conforms to the following statement from the ACMD; "Any compound, which is capable of producing a pharmacological response on the central nervous system or which produces a chemical response *in vitro* identical or pharmacologically similar to substances controlled under the Misuse of Drugs Act (1971)".[8, 11]

6.3. New/Novel Psychoactive Substances (NPS)

New (or Novel) Psychoactive Substances (NPS) is a term used to reduce the confusion being created in a fast-paced legal drugs market and the different states of legality of compounds throughout the world. There are nine principle categories of NPSs:[12] (1) synthetic cannabinoids (e.g. JWH073); (2) natural and synthetic

cathinones (the latter category describes the methylmethcathinones); (3) entactogens (e.g. MDA1); (4) novel stimulants (e.g. methiopropamine); (5) synthetic opioids (e.g. AH-7921); (6) novel tryptamine derivatives (e.g. dimethyltryptamine); (7) GABAeric drugs (e.g. gamma-hydroxybutyric acid); (8) dissociative (e.g. diphenidine); and (9) piperazines (e.g. meta-chlorophenylpiperazine).[13] See Figure 1 for structures.

Most NPSs are present in all facets of society and are currently a major problem facing prisons with between 60 – 90 % of prisoners taking “Spice”, a form of NPS.[14] There is also a strong link between nightclubs and NPS use by those aged between 16 - 24 who reported their NPS use.[15] This link could be potentially exploited by having all NPS samples tested and catalogued to allow tracking of current market trends. In addition, this will allow authorities to become more alert to when a new substance arrives on the market. There have been reports on testing of urine in nightclubs, which revealed the use of many drugs, both traditional and NPS; the detection of metabolites from drugs demonstrates that a portion of the attendees in the nightclubs were taking the drugs.[16] Smith *et al.*[17] highlight the uncontrolled nature of the NPS market where users are buying NPSs but the packet can contain something completely different.[16, 17] Therefore, for the safety of the public, both the metabolites that are produced within the human body as well as the drug itself need to be thoroughly understood in order to protect against the adverse effects within the human body but also protect users from the criminal exploitation element inherent with illegal drugs.

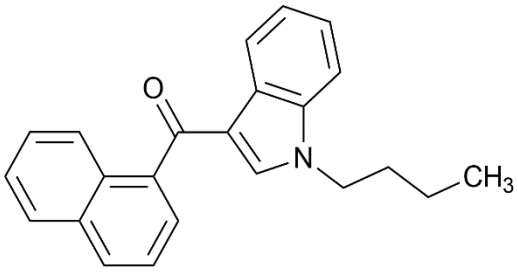

1) Sythetic cannabinods (JWH073)

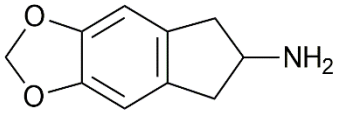

3) Entactogens (MDA1)

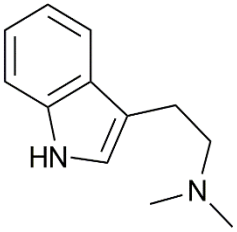

6) Novel tryptamine derivatives (dimethyltrypamine)

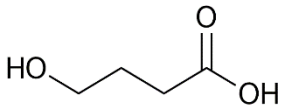

7) GABAeric drugs (gamma-hydroxybutyric acid)

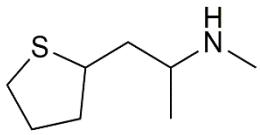

4) Novel stimulants (methiopropamine)

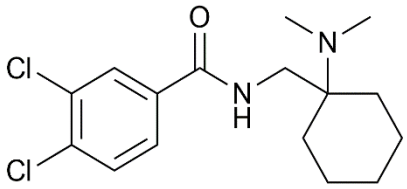

5) Syntetic opioids (AH-7921)

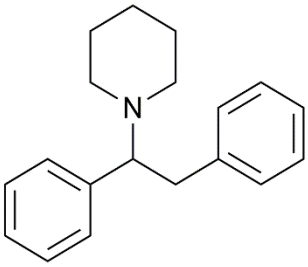

8) Dissociatives (diphenidine)

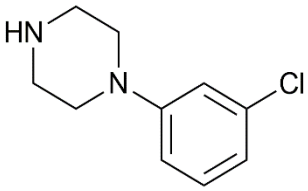

9) Piperazines (meta-chlorophenylpeprazine)

Figure 1 Structures of the common types of NPS.

6.4. Cathinones

The cathinone class of NPSs are structurally similar to the amphetamines. The main difference is the addition of the carbonyl bond to create a β-ketone. Cathinones can be natural or synthetic. Natural cathinones are extracted from the Khat plant (*Catha edulis*).[18] Synthetic cathinones are prepared in laboratories using chemical manipulation of the basic cathinone structure to create a new product. For example, the addition of a fluorine atom instead of the methyl group in mephedrone (4-methylmethcathinone) produces the derivative 4-fluoromethcathinone (4-FMC).

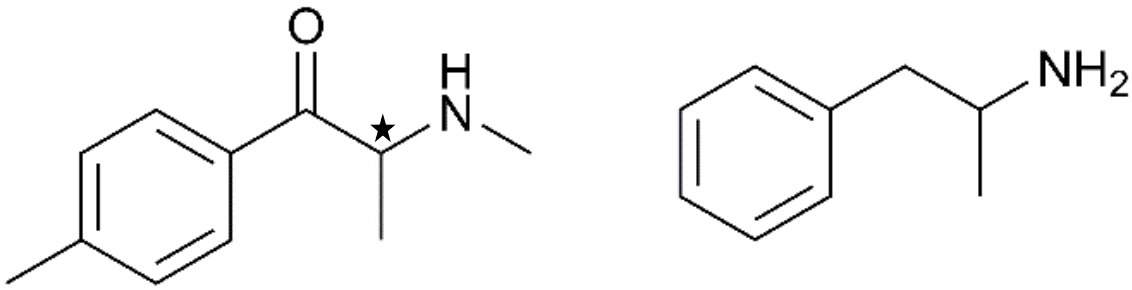

Figure 2 The chemical structure of 4-methylmethecathinone (**3**) (left) and amphetamine (right). The chiral centre on **3** is denoted by the star. The other regioisomers are analogous

Much research has been invested into the characterisation and detection of this class of NPS because of its historical prevalence over the years.[17] The cathinones are generally stereoisomeric and as such have (R)- and (S)- stereoisomers. However, with cathinones, the (S)-stereoisomer is the most potent within the human system. This theory is based on the (S)-stereoisomer being the most potent for cathinone, a closely related compound.[12] There is a risk that higher doses could be taken due to the induced tolerance developed from taking the drug. Online advice gives upto 75 mg as a dose for insufflation, but the reported amounts taken by repeat users is over 1 g.

One of the most prevalent cathinones in Europe is mephedrone and the cathinone class itself has been extensively studid since its emergence in 2010.[19, 20] The regioisomers of methylmethcatinone[21] are ring substituted cathinone structures. This NPS was developed to be substituted for the illegal drug Ecstasy.[17] Mephedrone was first reported in 2003.[12] In the UK four deaths were linked to mephedrone in 2010.[21] Ever since then, more and more drugs are being developed and sold as plant food or designer drugs. This allowed, until now, organised crime to bypass laws set in place to protect the public. According to the Office of National Statistics (ONS) and the Home Office there were an estimated 205 individuals using Mephedrone in the period 2013-2014 and an approximate 115 of these users were

16-24 year olds.[22] The data was collected from the household Crime Survey of England and Wales 2013/2014. This is a survey conducted every year since 1996 and has a high response rate of 72%.[23] An increase from 107 to 115 of 16 - 24 year olds reporting mephedrone use in the years 2012/2013 to 2013/2014 has prompted extensive study with a wide variety of characterisation techniques. Santali et al.[4] gave the first separation of a pure reference sample of mephedrone from common contaminants and cutting agents like paracetamol and benzocaine, along with other common drugs like cocaine.[4] The study also included, characterisation data for the compound, which included Ultra-Violet Visible Spectroscopy (UV-VIS) and Nuclear Magnetic Resonance (NMR). Power et al.[1] examined the spectral differences between the regioisomers of methylmethcathinone (Figure 3); 2-methylmethcathinone (compound 1), 3-methylmethcathinone (compound 2) and 4-methylmethcathinone (compound 3). The mass spectra for these compounds have been extensively studied using different techniques, for example Gas Chromatography (GC-MS)[1, 4] and Liquid Chromatography-High Resolution Mass Spectrometry (LC-HRMS).[4, 24, 25]

The most common regioisomer is 4-methylmethcathinone, also known as mephedrone. 4-MMC has chiral centres, which adds to the complexity of the activity within a human system.

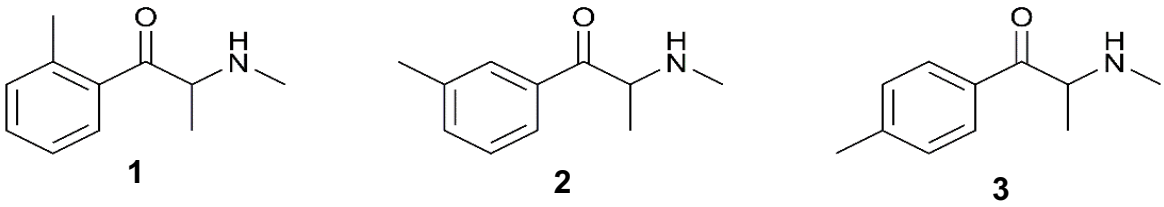

Figure 3 The chemical structure of 2-methylmethecathinone (1) (left) 3-methylmethecathinone (2) (middle) and 4-methylmethecathinone (3) (right)

These regioisomers are usually found as hydrochloride salts, however, 4-MMC has also been reported as a hydrosulfate and hydrobromide salt depending on the method of synthesis. The salt form used has an effect on the crystallinity of the compound, which is reflected in the melting points between the HCl, H_2SO_4 and HBr salts. The melting point of the hydrochloride salt of 4-MMC is 215.18°C[4] whereas the hydrobromide salt has a melting point of 205.25°C.[4] The recently characterised hydrosulfate salt has a melting point of 106.5°C.[26] The three salts both transform the freebased methcathinone from a yellow oil into the white or cream powder seen on the street.[4, 27] The hydrogen sulfate salt has been fully characterised using X-ray crystallography which determined the crystal system was monoclinic until 4.8 GPa where it became a triclinic system.[26]

The mass spectra for **1**, **2** and **3** have four major peaks. These are the most stable parts that the molecule can fragment into when analysed with an hard ionisation mass spectrometer like Electron Ionisation EI. The theoretical accurate mass of the parent ion on a ESI^+ MS is m/z = 178.1226 $[M\text{-}H^+]$[28] but when analysed using a hard ionisation technique such as electron ionisation (EI) the following fragmentation pattern will be seen: m/z=160 (loss of H_2O), 145 (CH_5N) and 130 (C_3H_9N).[4, 29]The mass at m/z=145 is the most stable form that the molecule can fragment into. These masses correlate to a series of losses of water (m/z=18), CH_5N (m/z=31) and C_3H_9N (m/z=59).[29]

The UV-VIS of 4-MMC was performed by Santali *et al*.[4] who used a range of solvents and conditions; absolute ethanol, water, HCl (0.1 M) and NaOH (0.1 M). The samples were recorded with a concentration of 9.1 $x10^{-4}$ g 100 mL^{-1}. The ethanol gave a wavelength of 259.5 nm (a = 0.735) whereas, the HCl and water gave 263.5 nm. This displays a bathochromic shift (a shift towards a longer wavelength) of 4 nm. The NaOH solution, however, gave a wavelength of 259.5 nm but an absorbance of 0.592 which is a hypsochromic shift (a shift towards a shorter wavelength) from that seen in ethanol. This could have been contributed to a change in ionisation. The HBr salts of **3** also displayed analogous results to that of the HCl salts.

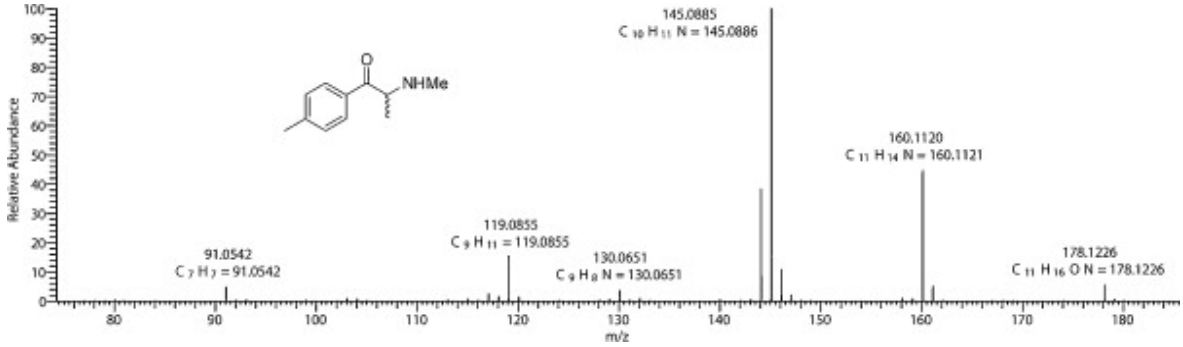

Figure 4 The fragmentation pattern observed with HRESIMS spectrum of (±)-mephedrone.HCl reproduced from Santali et al [4]

Power *et al*.[1] compared the regioisomers through ^{1}H NMR, FTIR and GCMS as a comparative study of the three regioisomers MMC.[1] The ^{1}H NMR was the clearest method for determining the regioisomer, through the aromatic region at 7 - 8 ppm. The 1,4-disubstituted aromatic gave two equivalent proton environments. The 1,3-disubstituited aromatic displayed two proton peaks and two peaks as a doublet and a triplet, whereas, the 1,2-disubstituted aromatic gave three peaks with an overlap of two doublets (Figure 5).

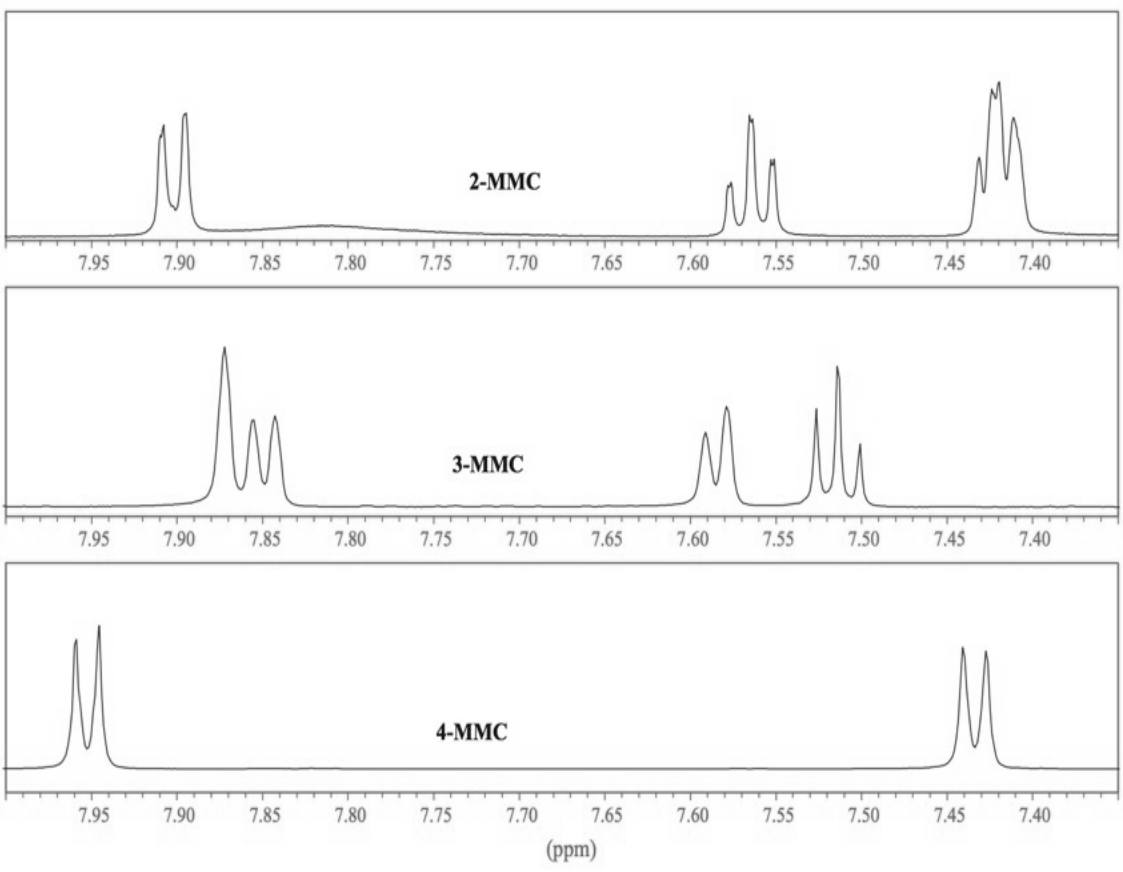

Figure 5 The aromatic region of the ^{1}H NMR reproduced from Power *et al.*[1]

This paper also studied the difference in the IR absorbance from a Fourier Transform Infra-Red Attenuated Total Reflectance (FTIR-ATR). There were differences in the C=O absorbance due to the steric effects of 3-MMC and 4-MMC, which had an absorbance of approximately 1865 cm^{-1} unlike 2-MMC, which had an absorbance nearer to 1696 cm^{-1}. The steric effects take place due to the position of the methyl group on the π ring and its proximity to the C=O bond. 2-MMC's methyl group is closer than either 3-MMC or 4-MMC and therefore has a greater hinderance on the C=O's adsorption of energy. The bands in the 675 - 900 cm^{-1} region also give details of the disubstitution. 2-MMC gives a strong absorbance at 752 cm^{-1}. 3-MMC gives three peaks at 894, 753 and 720 cm^{-1} whereas, 4-MMC has a peak at 827 cm^{-1}.

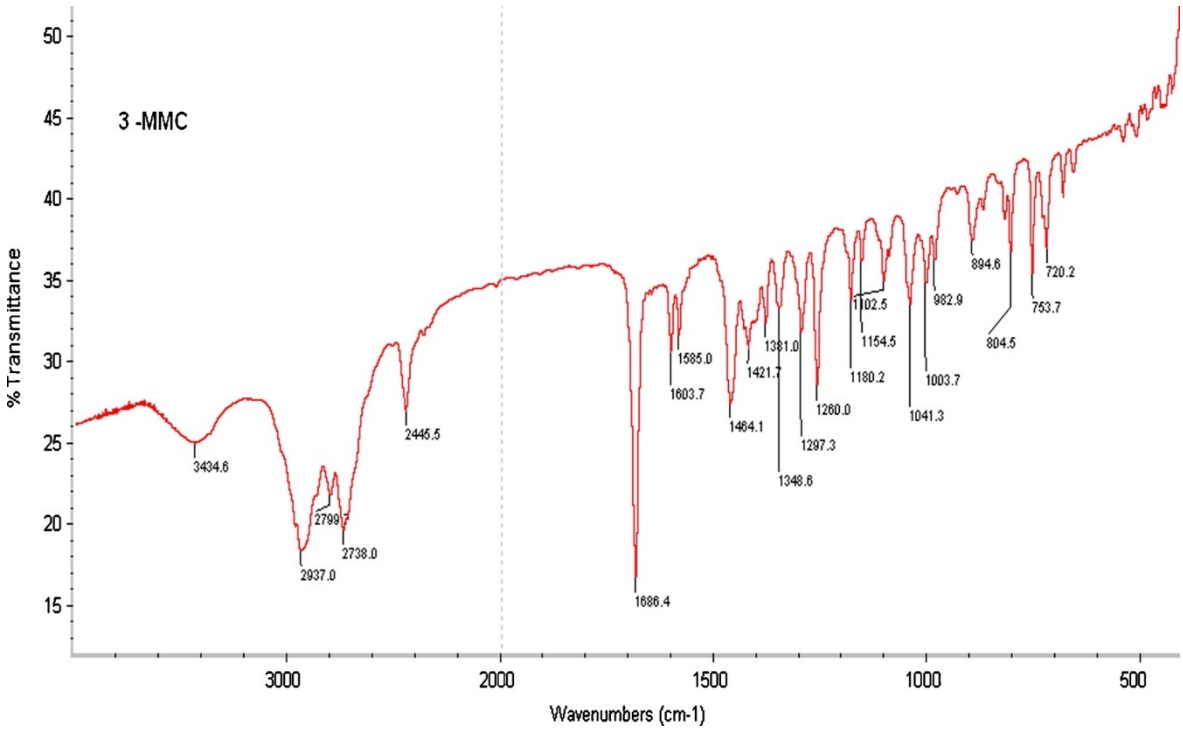

Figure 6. The FTIR spectra of 3-MMC reproduced from Power *et al*[1]

The chromatographic separation of mephedrone from other synthetic cathinones has been reported. High Performance Liquid Chromatography (HPLC) has been used mainly in the study of the metabolites of the drugs. The HPLC is usually coupled to HRMS and a variety of modes are used. One of these is Hydrophilic Interaction Liquid Chromatography (HILIC) to separate the synthetic cathinones taken from rat brain tissue.[30] The coupling of the HPLC to a HRMS allows for a more sensitive method with lower LODs and LOQ when compared to non-mass spectrum based detection. With the HRMS used as a detector the LOD was 5 ng mL^{-1} for mephedrone and the LOQ was 10 ng mL^{-1}.[30] This compared to a 260 ng mL^{-1} for LOD and 970 ng mL^{-1} LOQ, which came from a reverse phase HPLC method with a Diode Array Detector (DAD).[4] The difference in LOQ and LOD can be attributed to the detection method used but also the suitability of HILIC for MS.[3] The separation of the chiral R and S enantiomers has been conducted by Perera *et al.*[31] and by

Mohr *et al.*[32] who successfully separated the stereoisomers using a range of chiral HPLC columns. Taschwer *et al.*[33] has also performed a chiral separation of the MMC regioisomers. However, in this instance a cellulose column was used with a mobile phase of organic solvents. The method achieved a baseline resolution with 40 of the 43 samples studied and also achieved a >2 resolution between 3-MMC and 4-MMC enantiomers, but failed to fully resolve the enantiomers of 2-MMC. The t_R for 4-MMC was 11.62 and 14.89 minutes, for 3-MMC 12.33 and 13.65 minutes and for 2-MMC 11.89 and 13.91 minutes.

6.5. Metabolites

Metabolites are the products of biotransformations within the body with the purpose of allowing the body to excret both endogenous compounds and xenobiotics: such as drug molecules.[24, 34] The metabolism of drugs can undergo many different reactions, for example oxidation and reduction. The compounds undergo metabolism through the use of enzymes. The primary enzyme involved in the phase I metabolism of mephedrone is P450 cytochrome 2D6 (CYP2D6),[24, 34, 35] found in the liver and is responsible for the metabolism of 25% of the clinical drugs used today.[34]

Drug metabolism involves numerous biotransformations with the ultimate aim of making the drug absorbable. There are many ways this can be done. However, this is mainly split between two different phases. Phase I is the small changes to the structure of the drug to make it more hydrophilic therefore, allowing it to be absorbed by the body's defences. These small changes can take the shape of oxidation or reductions. Phase II is the conjugation of bigger hydrophilic compounds which overcome the hydroscopic nature of the drugs thereby allowing it to be excreted as waste.

The metabolites of mephedrone have been studied in both *in vivo* and *in vitro*. The studies have used both rat and human subjects and freshly isolated Sprague-Dawley hepatocytes.[2, 24] From these studies the biotransformation of mephedrone is via phase I and II pathways. The Phase I pathways uses simple reactions to transform the parent compound through the use of reduction, oxidation and reductive N-dealkylation.[24] The *in vitro* studies show a common mechanism with amphetamine where the predominant process is on the plasma membrane catecholamine transporters.[12] The *in vivo* study highlighted 10 metabolites after 4 hours of dosing.[2] This was split over the two phases in a ratio of 6:4.[2] The Phase II metabolites where broken down further into glucuronic acid based and succinic acid.[2] The conjugation of succinic acid is not typically seen, and it is expected to be a storage mechanism for the *nor*-mephedrone when it is subsequently hydrolysed. Further phase II transformation is the sulfation of mephedrone. This transformation, although expected, has not been observed. It is believed that this is due to the higher concentrations of the drug forcing the biotransformation into a glucuronidation pathway.[24] A transformation of interest is the direct reduction of the mephedrone to methyl-ephedrine.

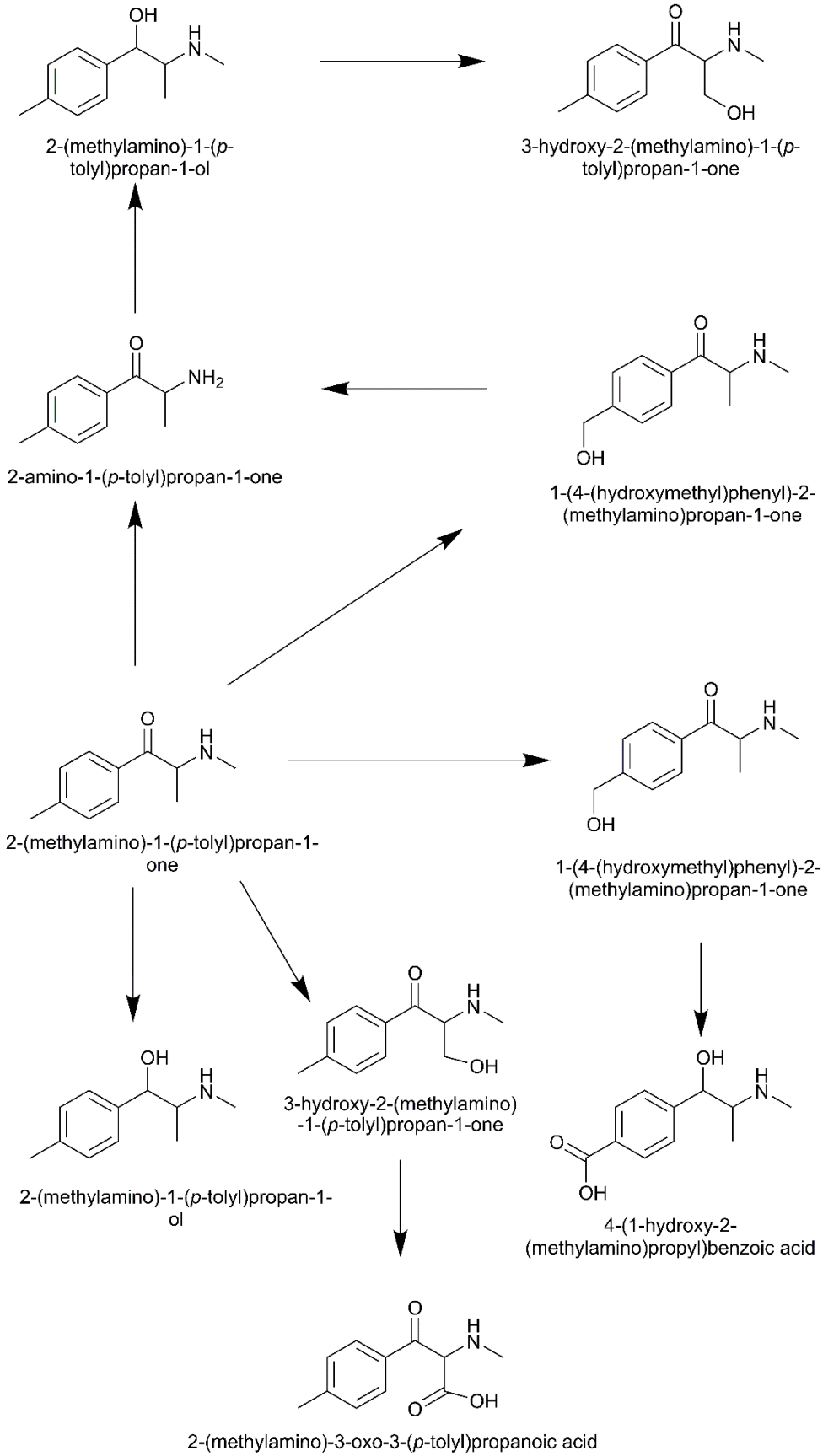

Figure 7 The phase one metabolic pathway of **4-MMC** reproduced from Pozo *et al.* [2] This was an *in vivo* study of 200 mg taken orally. Samples were then taken from urine after four hours.

The three metabolites to be studied in this project are 2-methylephedrine, 3-methylephedrine and 4-methylephedrine (Figure 8). These compounds are small and highly polar making them difficult to separate on a traditional reverse phase column, therefore, HILIC will be used to separate the all regioisomers of both methyl methcathinone and methylephedrine.

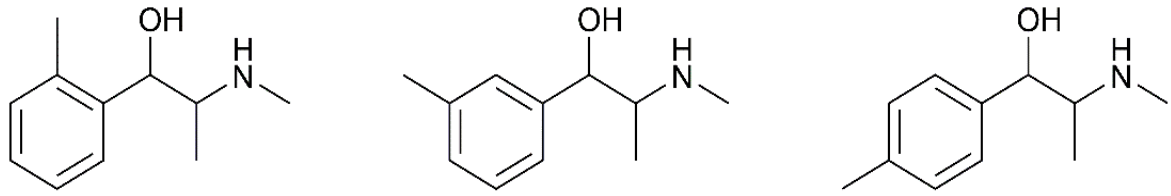

4 **5** **6**

Figure 8 The structures of 2-methylephedrine (**4**) (left). 3-methylephedrine (**5**) (middle). 4-methylephedrine (**6**) (right).

6.6. Hydrophilic Interactions LIquid Chromatography (HILIC)

Gregor *et al*. created the first HILIC method in 1951.[36, 37] Three years later the mechanism of HILIC separations, was proposed by Rückert and Samuelson.[36] The term HILIC, however, was not adopted until 1990, when Alpert used it for the first time.[37] For the next decade HILIC was not an active technique but in 2000 it started to become of interest to the scientific community again.[36]

The HILIC technique combines three popular liquid chromatography methods into a complementary mode for separating polar compounds. The separation of polar analytes can be difficult to achieve on Reverse Phase (RP) alone.[37] Normal phase, reversed phase and ion chromatography, each mode fulfils a key part of the HILIC mode, with RP giving the eluent, Normal Phase (NP) the adsorbent, and ion chromatography the type of compounds it will separate.[38]

The principal method of retention is liquid-liquid separation. Hydrophilic partitioning is the mechanism where the analyte, depending on its hydrophilic nature, will move

into the more stationary layers around the column packing.[38] Hydrogen bonding occurs when an electronegative element like nitrogen interacts in a dipole-dipole nature to form a bond between the water around the stationary phase and the analytes. For the HILIC mechanism, the hydrogen bonding allows the analyte to interact with the polar water layer and the stationary phase. The electrostatic interactions occur between the charged functional groups of a molecule and the charged parts of the column phase.[38]

The method relies upon layers of different concentrations of water and organic mobile phase forming around the stationary phase of the column. This forms a concentration gradient, which is the key to the separation process. The partitioning of the analyte into the correct layer depends on the ratio of the water and organic solvent. A ratio of less than 20% will create layers which cover around 12% of the pore volume of the stationary phase.[3] This is key as the interaction of the hydrophilic compounds with the static water rich layers is the main retention mechanism. By increasing the hydrophilic nature of the compounds the partitioning coefficient shifts so that it's weighted towards these fixed layers.[3] This then allows separation to occur.

This, however, is not the only method or interaction taking place with in the column. The analyte can undergo hydrogen bonding with the water layer, thus increasing its attraction with the more immobile layers.[3] The analyte can also experience electrostatic interactions with the stationary phase itself.[38, 39] For example, negatively charged sulfonate groups are likely to form electrostatic interactions directly with the analyte.[3]

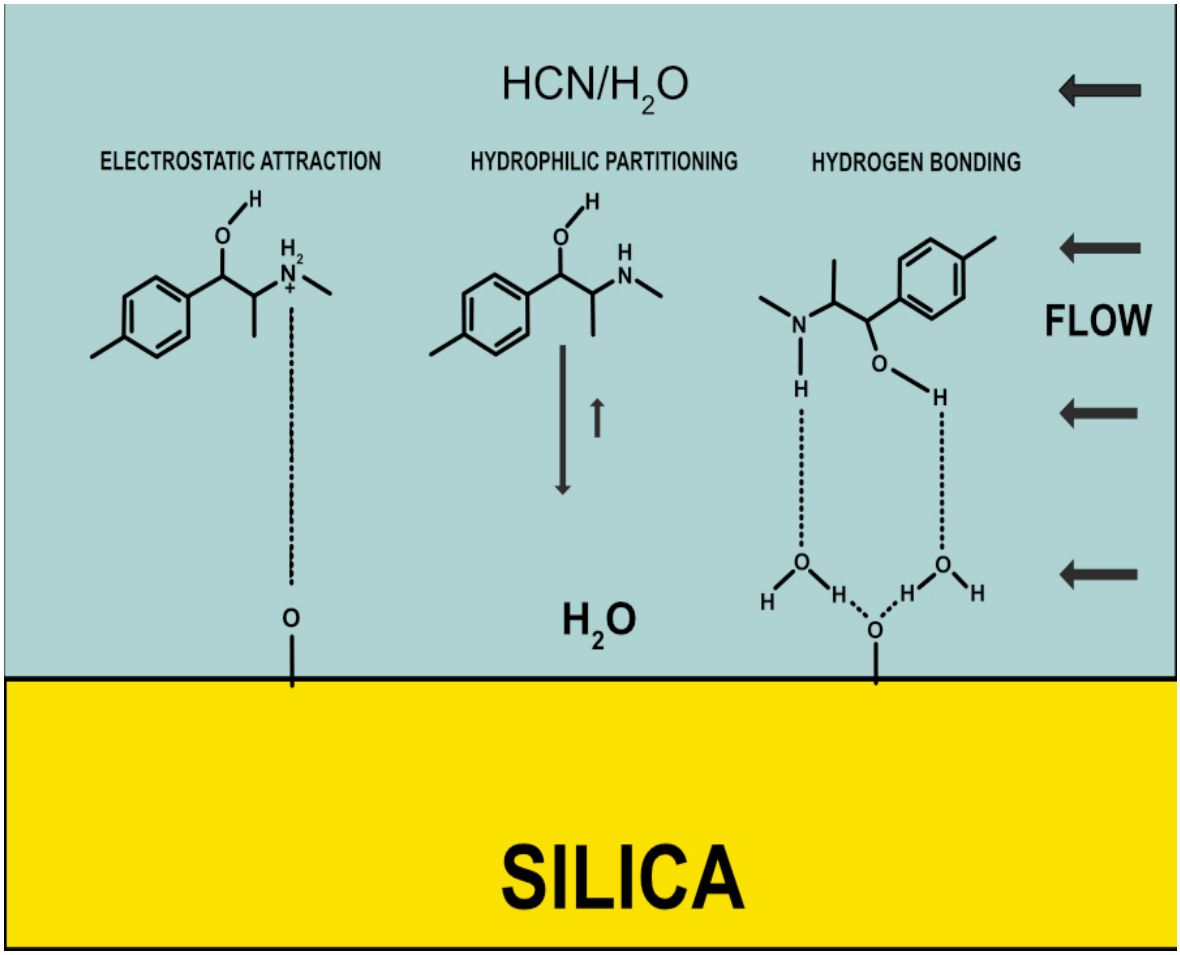

Figure 9 A diagram showing the proposed interactions involved in the separations in HILIC. The diagram also shows the layers formed in the HILIC mode. Redesigned from Buszewski. [3]

The proposed interactions for compounds **1 – 6** to interact with the HILIC mode will be the hydrophilic partitioning and hydrogen bonding as shown in Figure 9. This would be because of the two electronegative atoms present (nitrogen and oxygen). Others have used HILIC to facilitate the separation of the drug mephedrone and its' metabolites. **2** and **5** have also been separated using HILIC using a formic acid 0.05% / ammonium formate 10 mM and acetonitrile 0.05% formic acid mobile phase. These solutions were used on a gradient of 10 mM aqueous ammonium formate (containing 0.05% formic acid)-acetonitrile (containing 0.05% formic acid) [99:70% v/v] over 6.5 minutes. The HILIC mode has been applied to metabolite studies of mephedrone; Khreit *et al.,*[24] for example, has identified phase I and II metabolic pathways.[24] The method used aqueous formic acid 0.1% - acetonitrile (containing

0.01% formic acid). This method used a gradient which altered the aqueous formic acid from 20% to 80%. It also used an alternate ZIC-HILIC column (150 x 4.6 mm 5 µm). Li *et al.*[40] compared three different HPLC columns C18, phenyl and HILIC (Silica) for the separation of eleven cathinones.[40] Of the three, only the HILIC achieved full baseline separation of all eleven compounds, showing that for these smaller, polar compounds, HILIC is the primary choice of separation method.

6.7. Aims and Objectives

The need to detect an abused drug within a clinical / criminal setting, as well as its metabolites, is becoming important to allow a positive identification of a specific NPS drug being used. When the drug has biotransformed, the detection of its metabolites within blood and urine samples would allow drug takers to be identified. Therefore, it is the aim of this project to separate **1** - **6** in a single method, allowing a fast and practical means of separating and quantifying these compounds (and their reduced methylephedrines) within samples. To achieve this, HILIC mode will be used with a silica column to facilitate its eventual transfer onto LC-HRMS. The metabolites will be synthesised and will then be fully characterised to allow a whole understanding of the metabolites' chemical profile, allowing analytical methods to be applied for it detection.

7. Methods and Materials

7.1. Materials

All reagents were of commercial quality and were purchased from Sigma Adrich Gillingham, UK, Fisher Scientific Geel, Belgium and Alfar Asear Heysham, UK. The water used in the mobile phase was deionised using a millipore deioniser (resistance > 1 MΩ•cm). The acetronitrile was of HPLC grade from Fisher Scientific.

Compounds **1** – **3** (2-MMC, 3-MMC and 4-MMC) were obtained from Manchester Metropolitan University stock, which was synthesised (under Home Office licence) by Dr Sutcliffe following the method set out by Santali *et al.*[4]

7.2. Instrumentation

The NMR spectra were collected using a JEOL ECS-400 NMR with a frequency of 400 MHz for ^{1}H NMR and 100 MHz for ^{13}C NMR. The data was processed using the accompanying Delta software. The solvent used was d_6-DMSO with a sample target concentration of 26 mg mL^{-1}. Spectraa of compounds **1** - **3** were collected at an elevated temperature of 60°C as per the method reported by Santali *et al*.[4]

The HRMS was conducted on an Agilent 1250 / 6540 Liquid Chromatography High Resolution Mass Spectrometry Quadropole Time Of Flight (LCMS QTOF) using Electrospray ionization. This had a collision energy of 20 eV and was analysed in an acetonitrile and 1% formic acid mobile phase as an isocratic phase. The sample was directly injected into the mass spectrometer. The QTOF used a gas temperature of 325°C, a sheath gas temperature of 350°C, a gas flow of 5 L min^{-1}, a nebuliser pressure of 15 psig. The source was set with a Capiliary Voltage (VCap) of 4000 eV, a nozzle voltage of 500 V and the fragmentor was set to 15 eV.

The EI fragmentation pattern for each compound was observed using a Gas Chromatography-Mass Spectrometer (GC-MS) 6890 with a 5973 MS detector (Agilent Technologies). The samples were weighed out to possess a mass of 5 ± 0.5 mg. This was then dissolved into 1 mL of methanol and sonicated or 1 minute to create a final solution of 5 ± 0.5 mg ml^{-1}. A volume of 2 µL was injected in to the GC-MS. The injection port was a split/splitless inlet at a ratio of 20:1 and a temperature of 280°C. The column used was a HP5 MS 30 m x 0.250 mm and a film thickness of 0.25 µm. The oven program was 60°C for 1 minute, ramped to 280°C at 25°C per minute and held for 5 minutes. The transfer line was set to 300°C. The mass spectrometer was set to collect in the mass range of m/z = 50 – 250.

The FTIR- ATR experiment was performed using a Thermo Fisher Nicolet 360 with a ZnSe/Diamond crystal with a resolution of 4 cm^{-1} and 32 scans. The resulting data was processed with an ATR correction to compensate for absorbance seen by the crystal.

The UV-Vis experiments were collected on an Agilent 8453/8454 UV Vis spectrometer with a window of 190 nm to 400 nm, a path length of 1 cm and a slit of 1 nm. The samples were dissolved into both methanol and mobile phase (5 mM aqueous ammonium formate - acetonitrile [10:90% v/v]).

7.3. Synthesis of 2-methylephedrine

2-Methylmethcathinone (**1**) (0.29 g, 1.6 mmol) was added to methanol (20 ml) under a nitrogen atmosphere. Sodium borohydride (1.82 g, 44.93 mmol) was added slowly, followed by additional methanol (10 ml). This was left stirring for 24 hr under nitrogen. The reaction mixture was concentrated *in vacuo* and dissolved in deionised water (50 ml). This aqueous solution was then extracted using

dichloromethane (DCM) (3 x 75 ml). The organic fractions were combined and dried over anhydrous sodium sulphate, filtered and then washed further with DCM (20 ml). The filtrate was concentrated *in vacuo* to give a pale viscous yellow oil. The oil was dissolved in ethyl acetate (4 mL) and 4 M HCl in dioxane (4 ml) was added slowly. This solution was left stirring at room temperature for 1 hr. After completion of the reaction, the solution was triturated with acetone (3 x 75 ml), which produced an off white powder. This white powder was filtered and dried to give 2-methylephedrine.HCl (**4**) (0.20 g, 67% from **1**). Mpt. 198-199°C, ^{1}H NMR (400 MHz, d_6-DMSO) δ ppm = 9.11 (2H, s, N**H**$_2$), 7.49 (1H, d, Ar-**H**, *J* = 7.33Hz), 7.19 (3H, m, Ar-**H**), 6.01 (1H, s, β-C-**H**), 5.39 (1H, s, O-**H**), 3.21 (1H, m, α-C-**H**), 2.60 (3H, s, N-C**H**$_3$), 2.31(3H, s, AC-C**H**$_3$), 0.97 (3H, d, Ar-C**H**$_3$, *J* = 6.41 Hz). ^{13}C-NMR (101 MHz, d_6-DMSO) δ ppm = 139.67 (Ar-**C**), 134.56 (Ar-**C**),130.67 (Ar-**C**-H), 127.70 (Ar-**C**-H), 127.02 (Ar-**C**-H), 126.08 (Ar-**C**-H), 67.52(**C**-OH),57.41 (**C**-CH$_3$), 30.91 (**C**-NH$_2$), 19.20 (**C**H$_3$-Ar), 9.42 (**C**H$_3$). IR (ATR-FTIR) ν_{max} cm^{-1}: 3306 (OH), 2972 (C-H Stretch), 1580 (N-H Bending), 1473 (C=C Aromatic), 1423 (C=C Aromatic), 1410 (C=C Aromatic), UV (MeOH) λ_{max} = 210 nm (A = 0.67, c = 0.02 mg mL^{-1}). HRMS (ESI+, 20 eV) Theoretical $[M-H]^+$ =180.1383 m/z[41] Found $[M-H]^+$ = 180.1380 m/z (1.61ppm)

7.4. Synthesis of 3-methylephedrine

3-Methylmethcathinone (**2**) (0.32 g, 1.5 mmol) was added to methanol (20 mL) under a nitogen atmosphere. Sodium borohydride (1.88 g, 49.69 mmol) was added slowly, with additional methanol (10 mL). This was left stirring for 24 hrs under nitrogen. The reaction mixture was concentrated *in vacuo* and dissolved in deionised water (50 mL). This aqueous solution was then extracted using DCM (3 x 75 mL). The organic fractions where dried with sodium sulphate anhydrous, filtered

and then washed further with DCM (20 mL). The filtrate was concentrated *in vacuo* to give a pale viscous yellow oil. The oil was dissolved in ethyl acetate (4 mL) and 4 M HCl in dioxane (4 mL) was added slowly. This solution was left stirring at room temperature for 1 hr. After the completion of the reaction, the solution was triturated with acetone (3 x 75 mL), which produced an off white powder. This white powder was filtered gravimetrically and dried to give 3-methylephedrine.HCl (**5**) (0.18 g, 55.9 % from **2**) Mpt. 197-198°C, ^{1}H NMR (400 MHz, d_6-DMSO) δ ppm 9.03 (2H, s, N**H**$_2$), 7.26 (1H, m, Ar-**H**), 7.19 (2H, m , Ar-**H**), 7.09 (1H, d, Ar-**H**, J = 7.33 Hz) 6.10 (1H, s, β-C-**H**), 5.15 (1H, s, O-**H**), 3.31 (1H, m, α-C-**H**, J = 6.41 Hz), 2.61 (3H, s, N-C**H**$_3$), 2.32(3H, s, AC-C**H**$_3$), 0.92 (3H, d, Ar-C**H**$_3$, J = 6.41 Hz). ^{13}C NMR (101 MHz, d_6-DMSO) δ ppm 141.24 (Ar-**C**), 137.18 (Ar-**C**), 128.04 (Ar-**C**-H), 127.84 (Ar-**C**-H), 126.30 (Ar-**C**-H), 122.89 (Ar-**C**-H), 69.25 (**C**-OH), 59.13 (**C**-CH$_3$), 30.72(**C**-NH$_2$), 21.14(**C**H$_3$), 9.10 (**C**H$_3$-Ar). IR (ATR -FTIR) ν_{max} cm^{-1}: 3292 (OH), 2987 (C-H Stretch), 1608 (N-H Bending), 1421 (C=C Aromatic), 1469 (C=C Aromatic), 1589 (C=C Aromatic). UV (MeOH) λ_{max} = 211 nm (A = 0.71 , c = 0.02 mg mL^{-1}), HRMS (ESI+, 20 eV) Theoretical [M-H]$^+$ = 180.1383 m/z[41] Found [M-H]$^+$ = 180.1385 m/z (1.16 ppm)

7.5. Synthesis of 4-methylephedrine

4-Methylmethcathinone (**3**) (0.26 g, 1.5 mmol) was added to methanol (20 mL) under a nitrogen atmosphere. Sodium borohydride (1.7 g, 44.9 mmol) was added slowly, with additional methanol (10 mL). This was left stirring for 24 hrs under nitrogen. The reaction mixture was concentrated *in vacuo* and dissolved in deionised water (50 mL). This aqueous solution was then extracted with (3 x 75) mL of DCM. The organic fractions where dried with sodium sulphate anhydrous, filtered and then washed further with DCM (20 mL). The filtrate was concentrated *in vacuo*

to give a pale viscous yellow oil. The oil was dissolved into ethyl acetate (4 mL) and 4 M HCl in dioxane (4 mL) was added slowly. This solution was left stirring at room temperature for 1 hr. After the completion of the reaction, the solution was triturated with acetone (3 x 75 mL), which produced an off white powder. This white powder was filtered gravimetrically and dried to give 4-methylephedrine.HCl (**6**) (0.17 g, 66.5 % from **3**). Mpt. 201 – 203 °C, ^{1}H NMR (400 MHz, d_6-DMSO) δ ppm 9.01 (2H, s, N**H**$_2$), 7.27 (2H, d, Ar-**H**, J = 7.79Hz), 7.17 (2H, d, Ar-**H**, J = 7.79 Hz), 6.07 (1H, s, β-C-**H**), 5.14 (1H, s, O-**H**), 3.28 (1H, m, α-C-**H,** J = 6.41 Hz), 2.60 (3H, s, N-C**H**$_3$), 2.29(3H, s, AC-C**H**$_3$), 0.91 (3H, d, Ar-C**H**$_3$, J = 6.41 Hz). ^{13}C NMR (101 MHz, d_6-DMSO) δ ppm 139.21(Ar-**C**), 137.20 (Ar-**C**), 129.65(Ar-**C**-H), 126.65(Ar-**C**-H), 70.13(**C**-OH), 60.13(**C**-CH$_3$), 31.29(**C**-NH$_2$), 21.66(C-**C**H$_3$),10.10 (**C**H$_3$-Ar). IR (ATR-FTIR) vmax / cm^{-1}: 3349 (OH), 1559 (N-H Bending), 1422 (Ar C=C). 1437 (Ar C=C), 1470 (Ar C=C). UV (MeOH) λ_{max} = 212nm (A = 0.65, c =0.02 mg mL^{-1}) HRMS; Theoretical [M-H]+ = 180.1383[41] m/z, Found [M-H]+ = 180.1371 m/z (6.61ppm)

7.6. Presumptive testing of methylephedrine and methylmethcathinone

Five reagents were selected to test the metabolites with comparisons to the respective starting compound. These reagents were Simon's, Zimmerman's, Chen Kao, Lieberman's and Robadope. The selection of these reagents was based on the standard colour tests, recommended by the United Nations Office On Drugs And Crime which principally recommends the use of Zimmermann's reagent for the general detection of synthetic cathinones.[42] The method of preparing these reagents is stated below.

The presumptive tests were performed using a concentration of **1** – **6** at 10 mg mL^{-1} in deionised water. The colour test also required the use of a positive control, which

had the same functionality as the compounds being studied. The positive controls selected were methamphatime and amphetamine.

Robadope Test: comprises of three solutions - 2% aqueous sodium carbonate solution (10 mL); 1% aqueous sodium nitroprusside solution (10 mL); 50% ethanolic acetone solution (10 mL).[43]

Simon's Test: comprises of three solutions - 2% aqueous sodium carbonate solution (10 mL); 1% aqueous sodium nitroprusside solution (10 mL); 50% ethanolic acetaldehyde solution (10 mL).[44]

Zimmerman's Test: comprises of two solutions - 1% solution 1,3-dinitrobenzene in methanol (10 mL); 15% aqueous potassium hydroxide solution (10 mL).[43]

Liebermann's Test: 10% w/v sodium nitrite in concentrated sulfuric acid (10 mL).[44]

Chen-Kao Test: Comprises of three solutions - 1% v/v aqueous acetic acid (10 mL); 1% aqueous copper (II) sulfate solution (10 mL); 8% aqueous sodium hydroxide solution (20 mL).[44]

7.7. Mobile phases used in the chromatography experiments.

The mobile phases were made up to the correct volumes and concentrations and mixed together in the final container (see Table 2). The resulting solution was then filtered and degassed. The final volume of all solutions was 2 L.

Table 2 The mobile phases and their make-up used for the method development and the validation of the HILIC methods.

Mobile phase	Concentration and volume of aqueous ammonium formate	Volume of Acetonitrile	Resulting ratio of solvents	Final concentration of aqueous ammonium formate
A	50 mM in 200 mL	1800 mL	10:90% v/v	5 mM
B	50 mM in 100 mL	1900 mL	5:95% v/v	5 mM
C	50 mM in 60 mL	1940 mL	3:97% v/v	5 mM
D	400 mM in 100 mL	1900 mL	5:95% v/v	20 mM

7.8. Preparation of the calibration standards.

The standards were prepared to a maximum of 5% aqueous content and 95% acetonitrile in a stock solution of 100 and 50 μg mL^{-1} and sonicated for 5 minutes before being diluted to the desired concentrations of 50, 40, 20, 10 and 5 μg mL^{-1} for compounds **4** - **6** and 25, 20, 10, 5, and 2.5 μg mL^{-1} for compounds **1** - **3** with acetonitrile.

7.9. Separation of the methylmethcathinones isomers

The separation of the regioisomers was conducted following the method set out by Khurana.[45] This was performed with mobile phase B with the parent compounds (methylmethcathinones). This method worked in the separation of the all three regioisomers and was used as the starting point for the separation of the parent drug and their metabolites.

7.10. Validation of the separation of methylmethcathinone and methylephedrine

The HPLC method of separation of the **1** - **3** and the reduced methylephedrines **4** - **6** was performed in HILIC mode with a mobile phase composition of 5 mM aqueous ammonium formate - acetonitrile [10:90% v/v]. The column was Hichrom Ace 5 SIL (ACE-127-1546) 150 x 4.6 mm with a particle size of 5 µm. The HPLC was set to run at 30°C with a flow rate of 1 mL min^{-1}. The DAD was set to record all spectra with 215 nm and 254 nm as the target wavelengths. The autosampler was set to inject 20 µL of sample.

The HILIC method was validated as per the International Conference for Harmonisation (ICH) guidance.[46] The following parameters were studied: linearity, precision, accuracy, LOD and LOQ. The linearity and precision were studied using five replicate injections of calibration standards. The %RSD was calculated for each sample. Accuracy, or percentage recovery, was performed on samples prepared in acetonitrile. The standards were prepared in duplicate over a working range of 80% - 120% using 20 and 10 µg mL^{-1} as the target concentration for **4** - **6** and **1** - **3** respectively. Limits of detection and quantification were calculated from the standard deviation of the response and the slope of the five calibration standards.

8. Results and Discussion

8.1. NMR of 2-methylephedrine

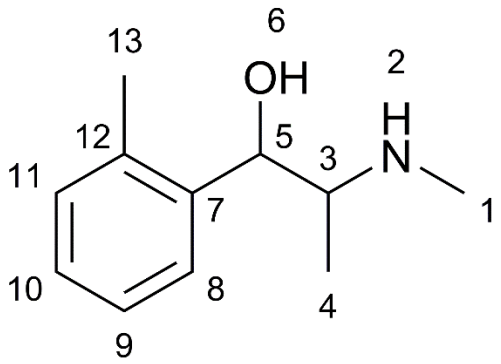

Figure 10 labelled structure of **4**

Table 3 Summary of the ^{13}C and ^{1}H NMR data of **4** in d_6-DMSO.

Shift ^{1}H (ppm)	Shift ^{13}C (ppm)	Position	^{1}H NMR Multiplicity	*J*-Value (Hz)
9.12	-	2	br s	-
7.49	127.02	8	d	7.33
	126.08	10		-
7.14 – 7.25	127.70	9	m	-
	130.67	11		-
5.36	67.52	5	s	-
6.02	-	6	br s	-
3.21	57.41	3	s	-
2.60	30.91	1	s	-
2.32	19.20	13	s	-
0.97	9.42	4	d	6.60
-	139.67	7	s	-
-	134.56	12	s	-

Compounds **4**-**6** differ only in terms of where the methyl group is postioned on the aromatic ring. For **4**, the methyl group is positioned in the *ortho* position. It is observed in the ^{1}H NMR spectrum at 2.32 ppm as a singlet. This affects the symmetry of the ring system and thus the chemical shifts of the nuclei, as well as their coupling constants. The methyl attached to the amine group is observed at 2.60 ppm; in the ^{1}H-^{13}C HMQC spectrum, a cross peak is observed to a carbon environment at 30.91 ppm. This environment is more deshielded than the methyl group of the aromatic ring, due to it being bonded to nitrogen. The carbon in this environment is located at 19.20 ppm in the $^{13}C\{^{1}H\}$ NMR spectrum. The other methyl group (located at postion (4)) is the most shielded environment as the carbon signal occurs at 9.42 ppm. The ^{1}H NMR signal is split in to a doublet, with a coupling constant of 6.60 Hz. In the ^{1}H-^{1}H COSY NMR spectrum, this peak shows a cross peak to a signal at 3.21 ppm, which integrates to one in the ^{1}H NMR spectrum. This peak is therefore the proton at postion (3). This deduction is further reinforced by this signal showing a second cross peak to the signal at 5.36 ppm, which again integrates to one in the ^{1}H NMR spectrum. The signal at 5.36 ppm is due to the single proton located at postion (5). This signal also shows a much weaker cross peak to the broad peak at 6.02 ppm. This latter signal is thus the alcoholic proton present in the molecule. The other much broader peak observed at 9.12 ppm in the ^{1}H NMR spectrum is, therefore, the amine proton.

Upon inspection of the ^{1}H-^{1}H NOESY experiment (Figure 13) there is no visible exchange between the OH and the NH protons. The reason this has not been observed may be due to the interaction of these two centres being weaker than that

observed with **5**–**6.** This could be weaker due to the presence of the methyl group being in the *ortho* position as oposed to that of *meta* or *para*.

When looking at all three regioisomers of methylephedrine there are great similarities in the spectra, however, there are also a few differences allowing for each isomer to be differentiated. This is apparent in the ^{1}H NMR spectra, in particular the difference in the aromatic part of the spectra (positions 7–12); the chemical shifts of these signals are recorded in Table 3. Although three of the environments possess signals that overlap, a single environment is observed as a doublet at 7.49 ppm with a ^{3}J ^{1}H-^{1}H coupling of 7.33 Hz. This is typical of a 3-bond coupling and is seen in compounds **5**–**6**.

When comparing the compounds **4**-**6** to the starting materials **1**-**3,** the spectra have the same similarities in terms of the aromatic region but a difference is observed in the aliphatic region due to the additional proton signal at 6.02 ppm in the ^{1}H NMR, which arises from the reduction of the carbonyl to the alcohol. This is also validated by the ^{13}C NMR spectrum due to the loss of the peak at 195 ppm, which corresponds to the carbonyl carbon being reduced.

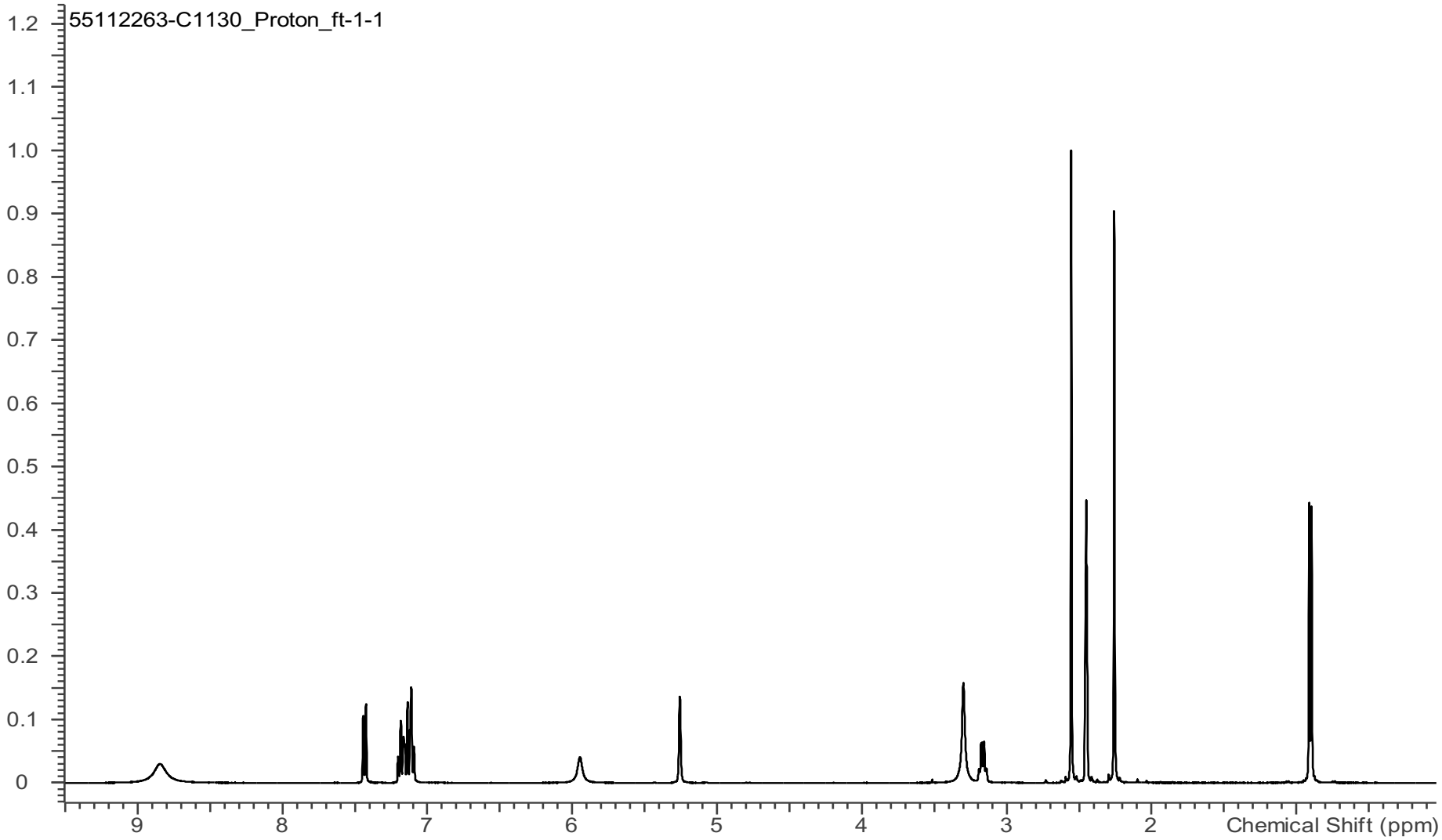

Figure 11 ^{1}H NMR spectrum of **4** in d_6-DMSO

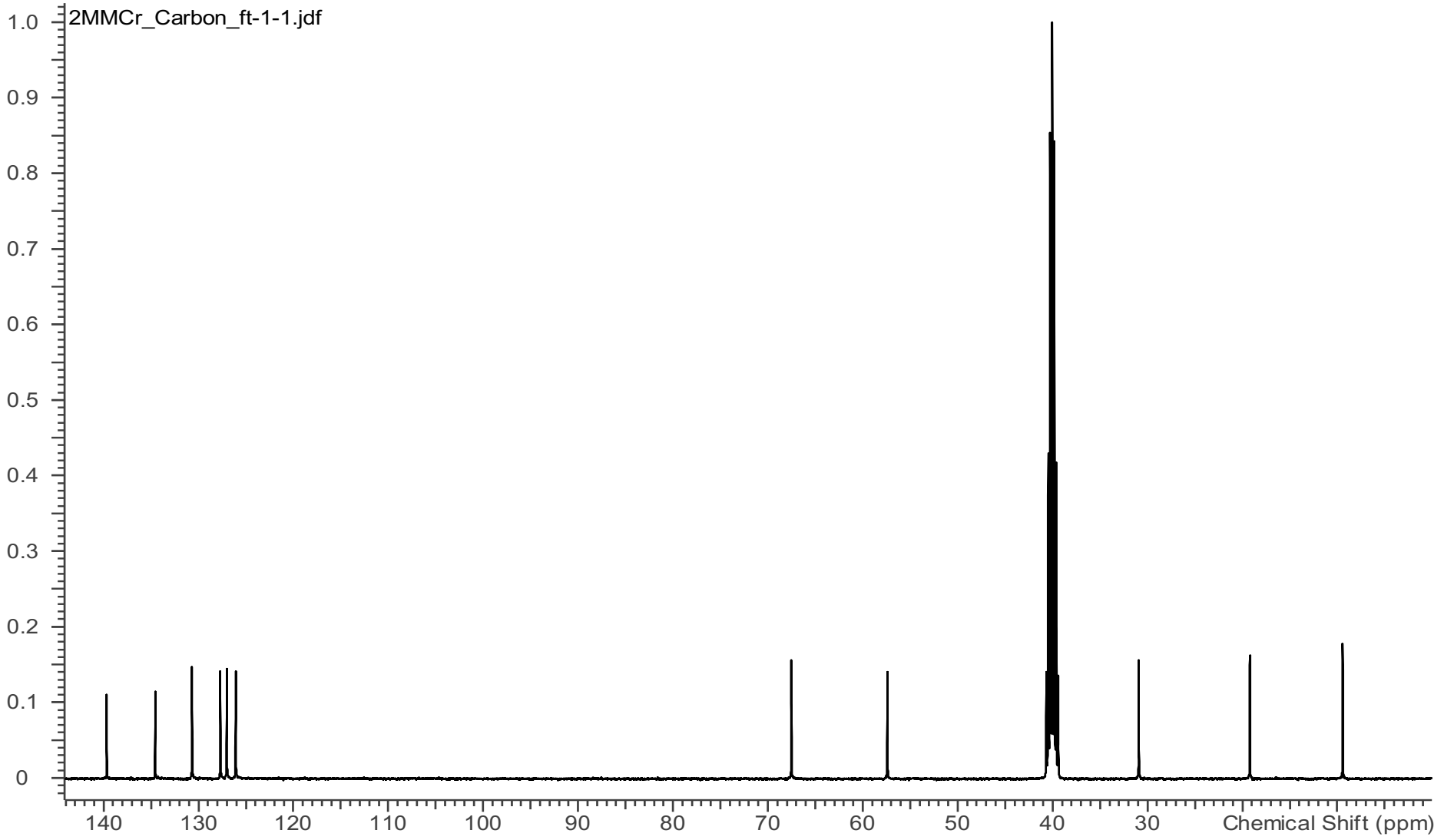

Figure 12 ^{13}C NMR spectrum of **4** in d_6-DMSO

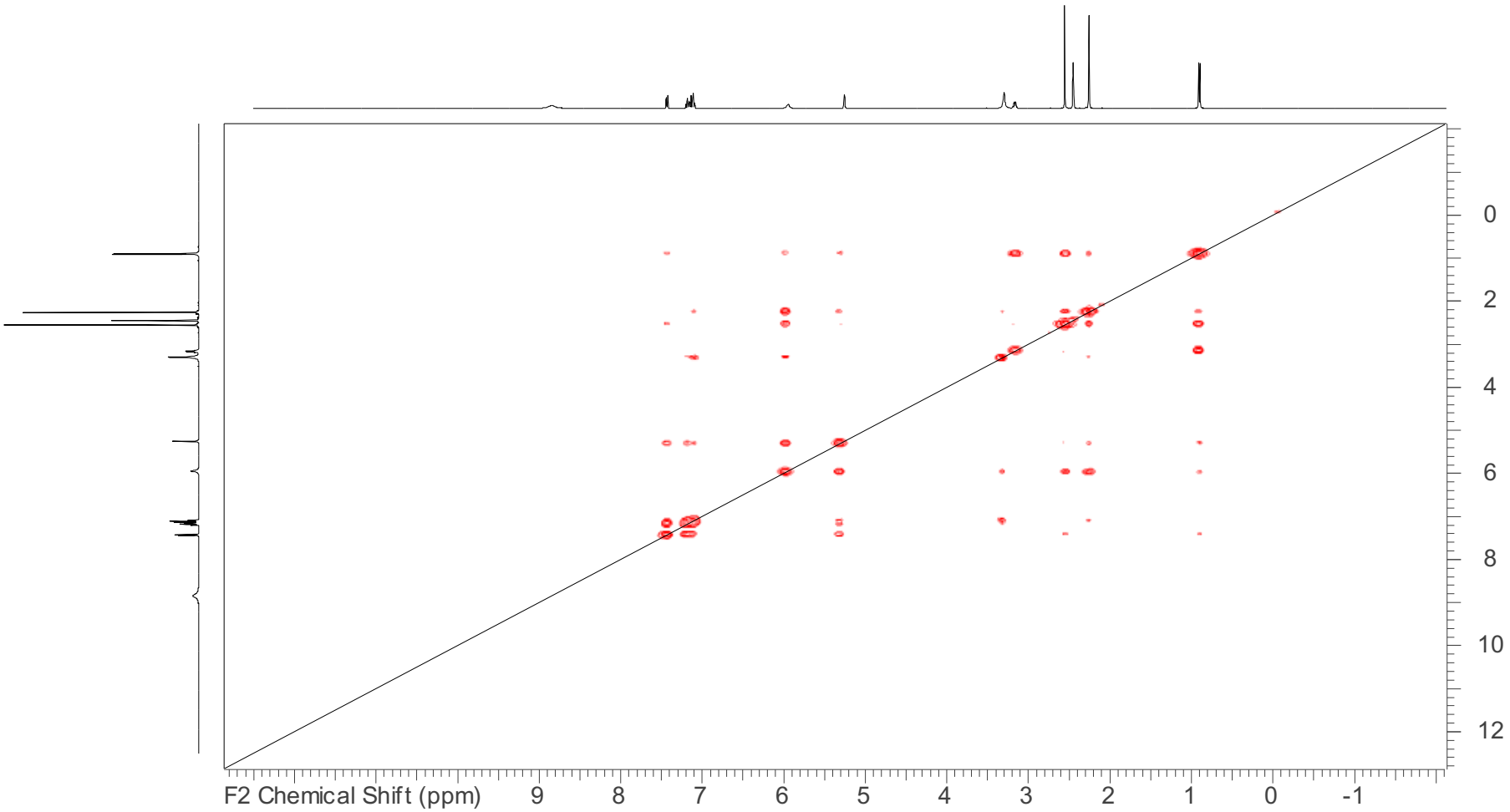

Figure 13 The ^{1}H-^{1}H COSY spectrum of **4** in d_6-DMSO.

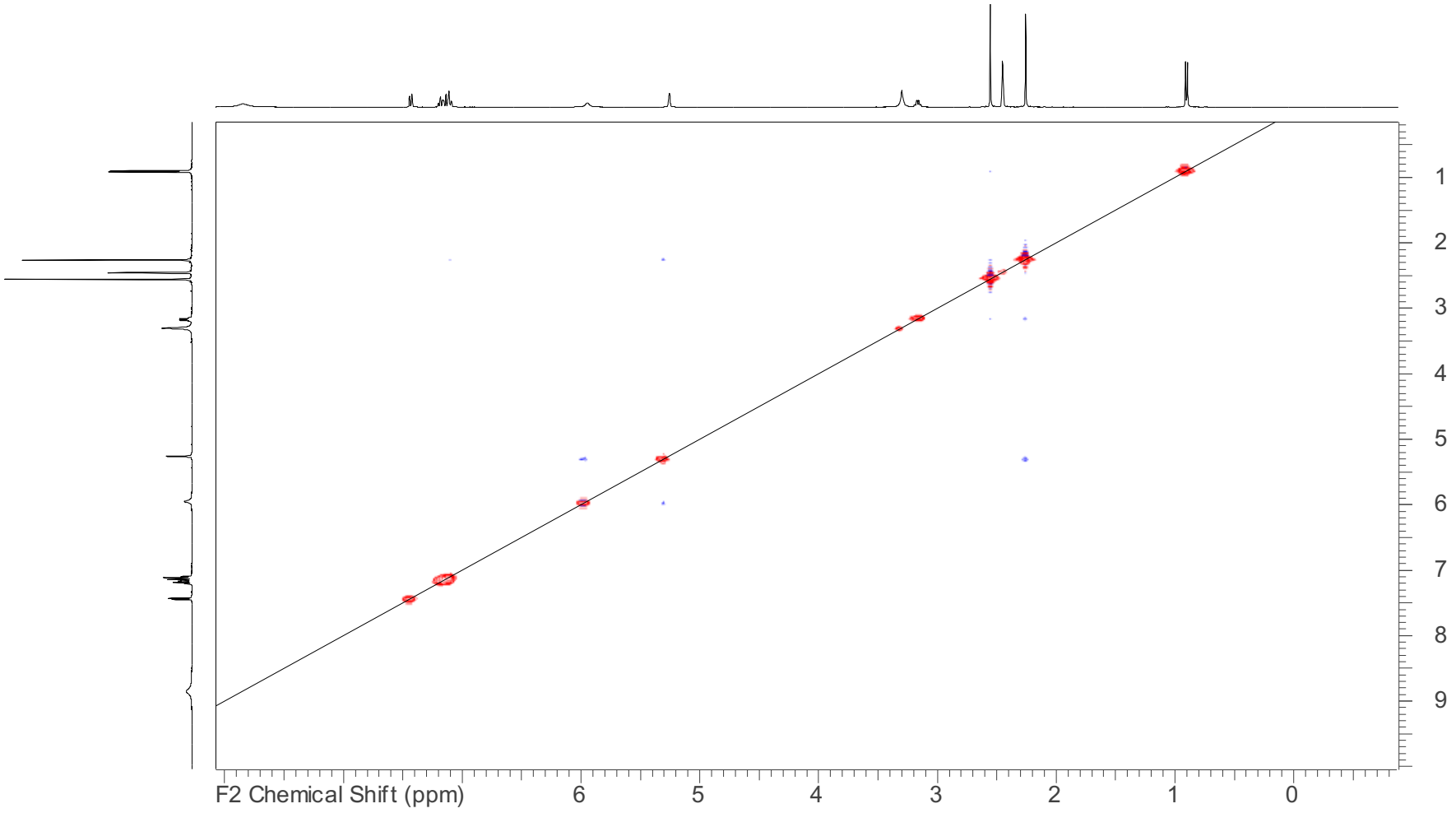

Figure 14 The ^{1}H-^{1}H NOESY of **4** in d_6- DMSO

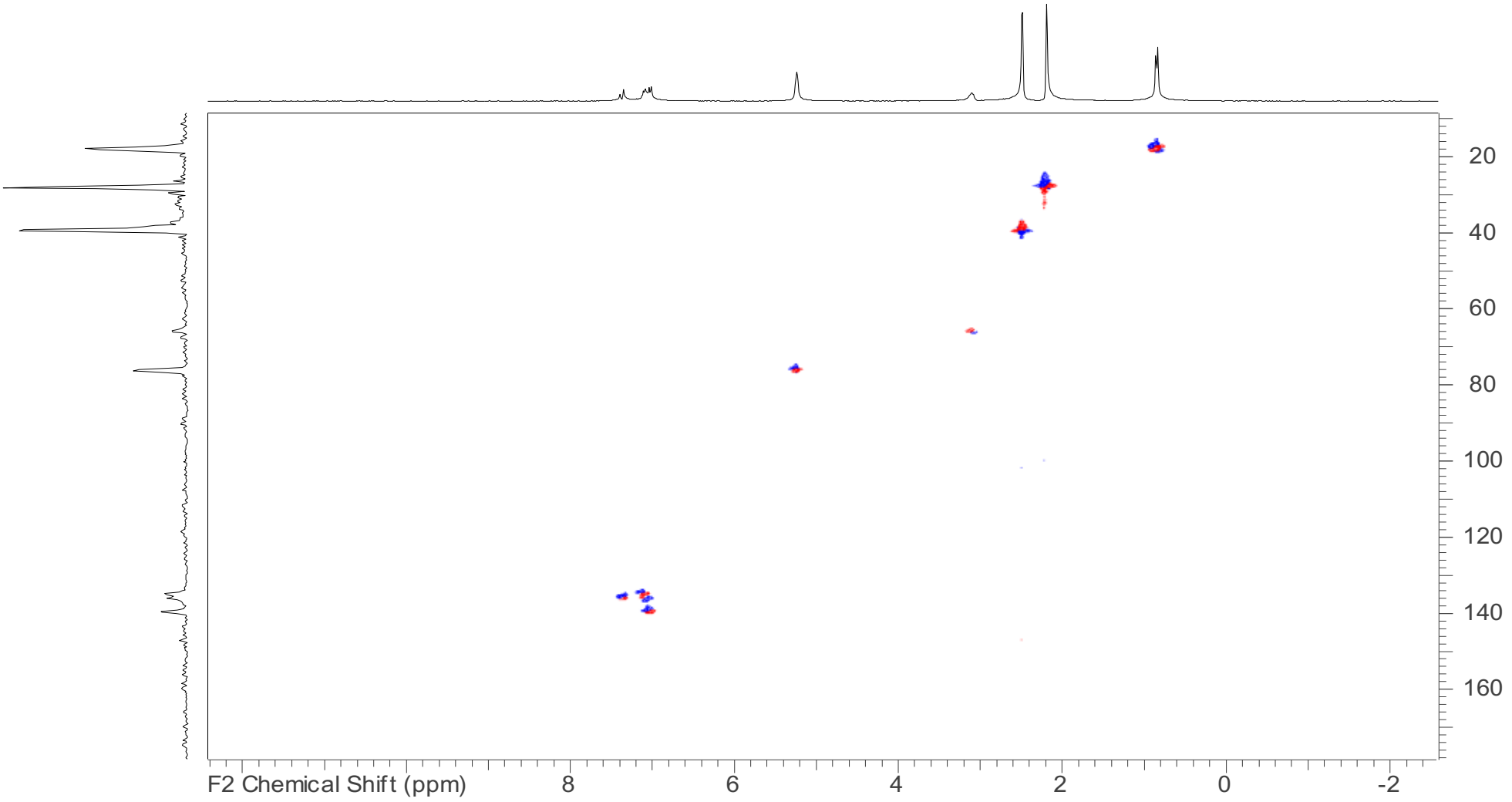

Figure 15 The ^{1}H-^{13}C HMQC of **4** in d_6- DMSO

8.2. NMR of 3-methylephedrine

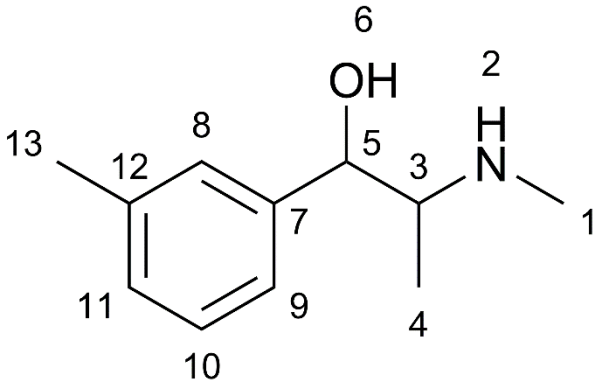

Figure 16 labelled structure of **5**

Table 4 Summary of the ^{1}H and ^{13}C NMR data of **5** in d_6-DMSO.

Shift ^{1}H (ppm)	Shift ^{13}C	Position	^{1}H NMR	*J*-Value (Hz)
9.03	-	2	br s	-
7.24 - 7.28	128.04	8	m	-
7.17 - 7.20	122.89	10	m	-
	126.30	9	d	7.33
7.09	127.84	11	s	-
6.10	-	6	br s	-
5.15	69.25	5	s	-
3.31	59.13	3	s	-
2.61	30.72	4	s	-
2.32	21.14	13	s	-
0.92	9.10	1	d	6.41
-	137.18	7	s	-
-	141.24	12	s	-

3-methylephedrine (**5**) is similar in most respects to **4** and **6**, however, the difference in the spectra arises from the different environments of the aromatic protons. The change of the methyl group from being *ortho* to *meta* has altered the symmetry within the aromatic ring meaning instead of two separate proton environments being seen there are now three. Looking at the ^{1}H-^{1}H COSY spectrum of compound **5** the peak at 2.30 ppm is connected to the peaks at 7.08 to 7.25 ppm. This shows that the methyl group at position (13) is interacting with all environments on the aromatic ring. The ^{1}H-^{1}H COSY also has two peaks at 7.08 and 7.18 ppm connected to the peak at 6.10 ppm, which corresponds to the proton attached to position (6). Looking at the absence of any coupling in the ^{1}H-^{1}H COSY, the peak at 7.25 ppm does not couple to anything other than the methyl group at position (13), indicating that the peak corresponds to the proton at position (11) as any other proton environment is more than $^{3}J_{HH}$ away. For the rest of the molecule the ^{1}H-^{1}H COSY demonstrates that the OH is coupling with the ^{1}H at position (5) but also the proton at (3). The proton at position (3) also shows a COSY interaction to CH_3 attached to the NH_2. The ^{1}H–^{13}C HMQC allowed for the assignment of the carbon spectra in Table 4. When comparing the peaks in the aromatic region, the ^{1}H – ^{13}C HMQC showed that there were two ^{13}C peaks correlating with the multiplet at 7.17 – 7.20 ppm which integrates to two protons. Thus, these protons must be two CH environments due to the 1:1 ratio of ^{1}H:^{13}C.

The ^{1}H–^{13}C HMQC also reveals that the lack of cross-peaks for carbon nuclei at 137.18 and 141.24 ppm meaning that these peaks belong to the non-hydrogen bearing carbons and are hence quaternary.

Looking at the ^{1}H-^{1}H NOESY (Firgure 19) there is evidence of an exchange process between the proton on the nitrogen (9.22 ppm) to that of the oxygen (6.02 ppm). This exchange is not observed in **4**.

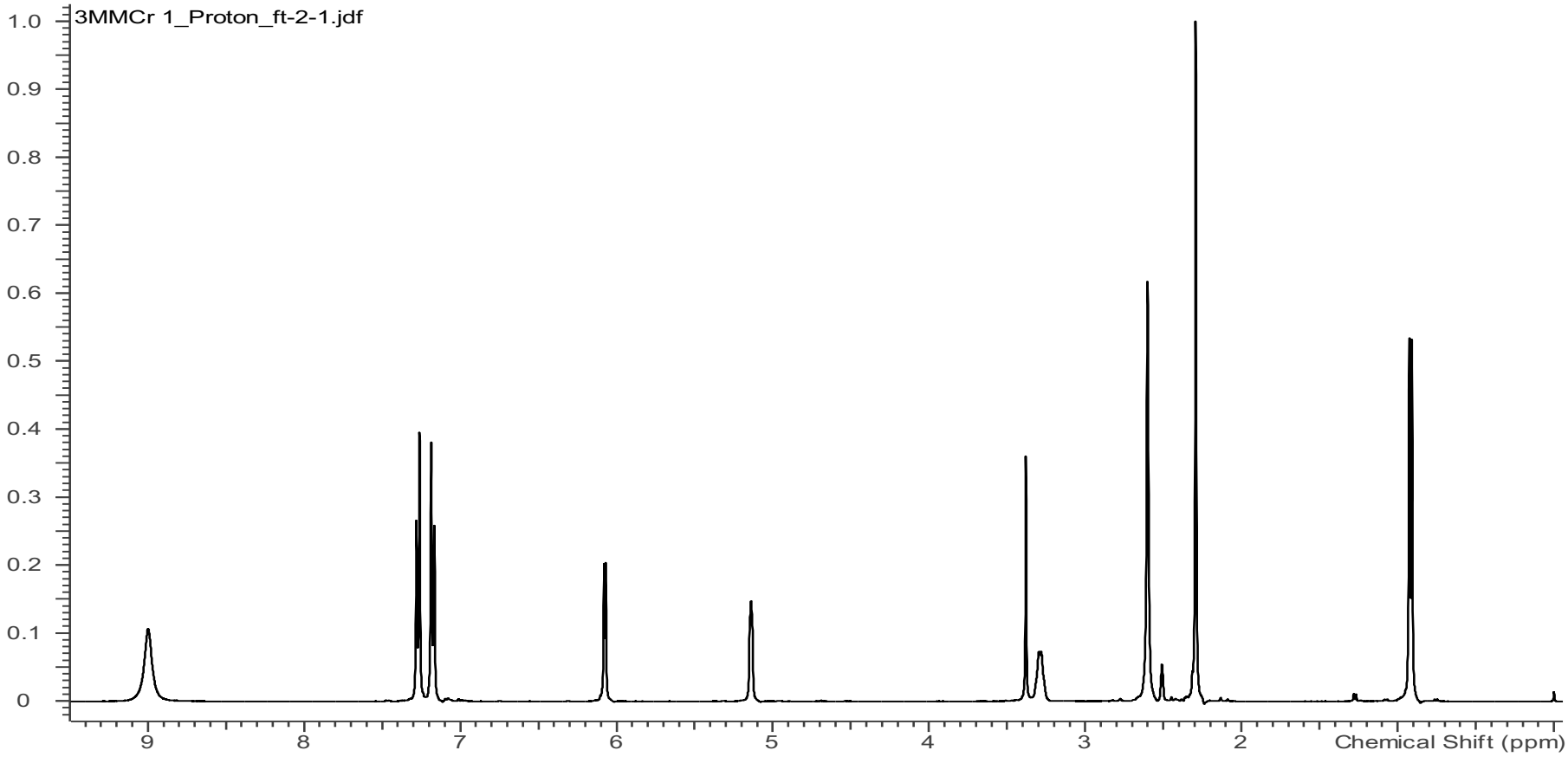

Figure 17 The ^{1}H Spectrum of compound **5** in d_6-DMSO

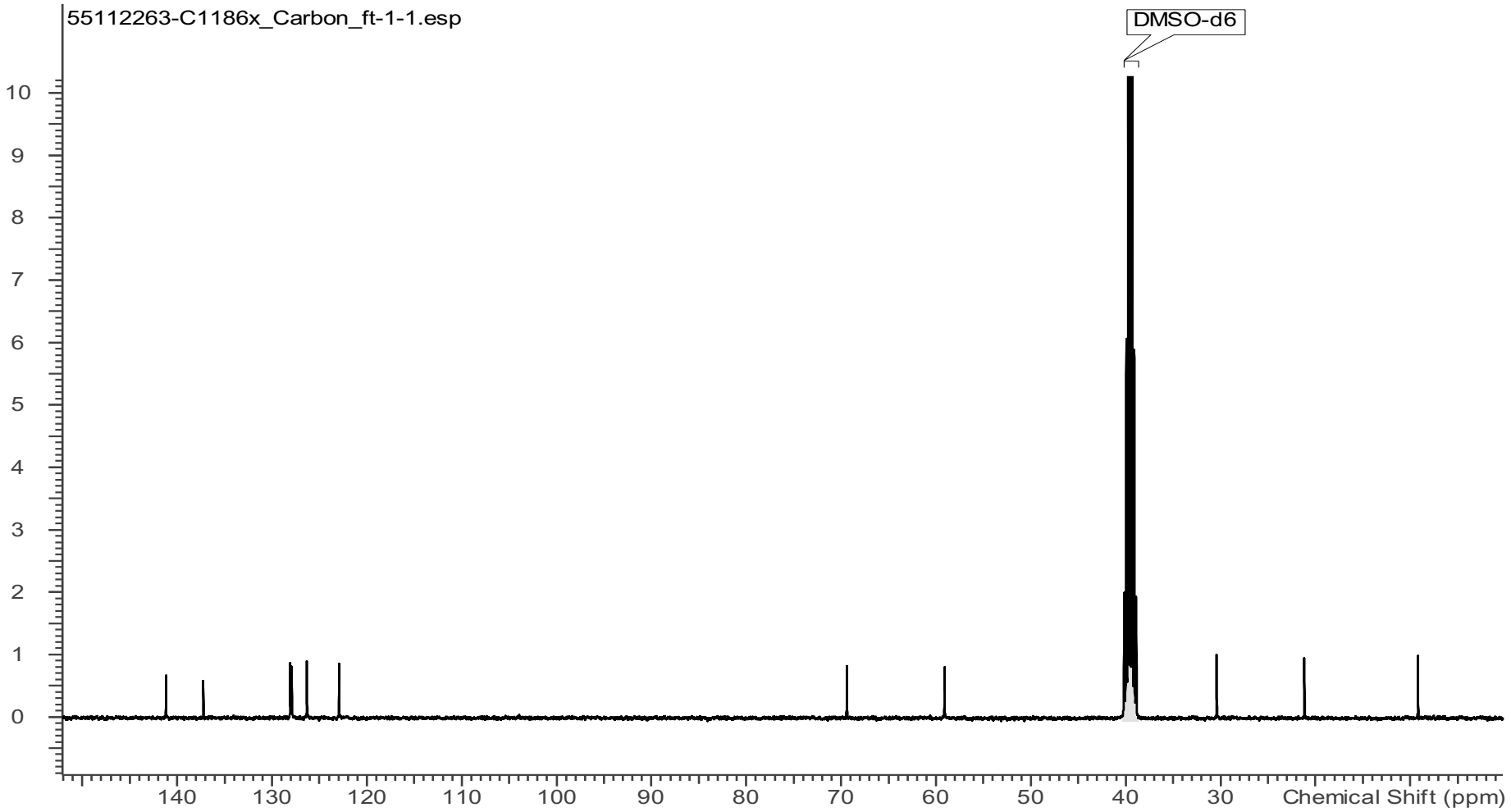

Figure 18 ^{13}C spectrum of compound **5** in d_6-DMSO.

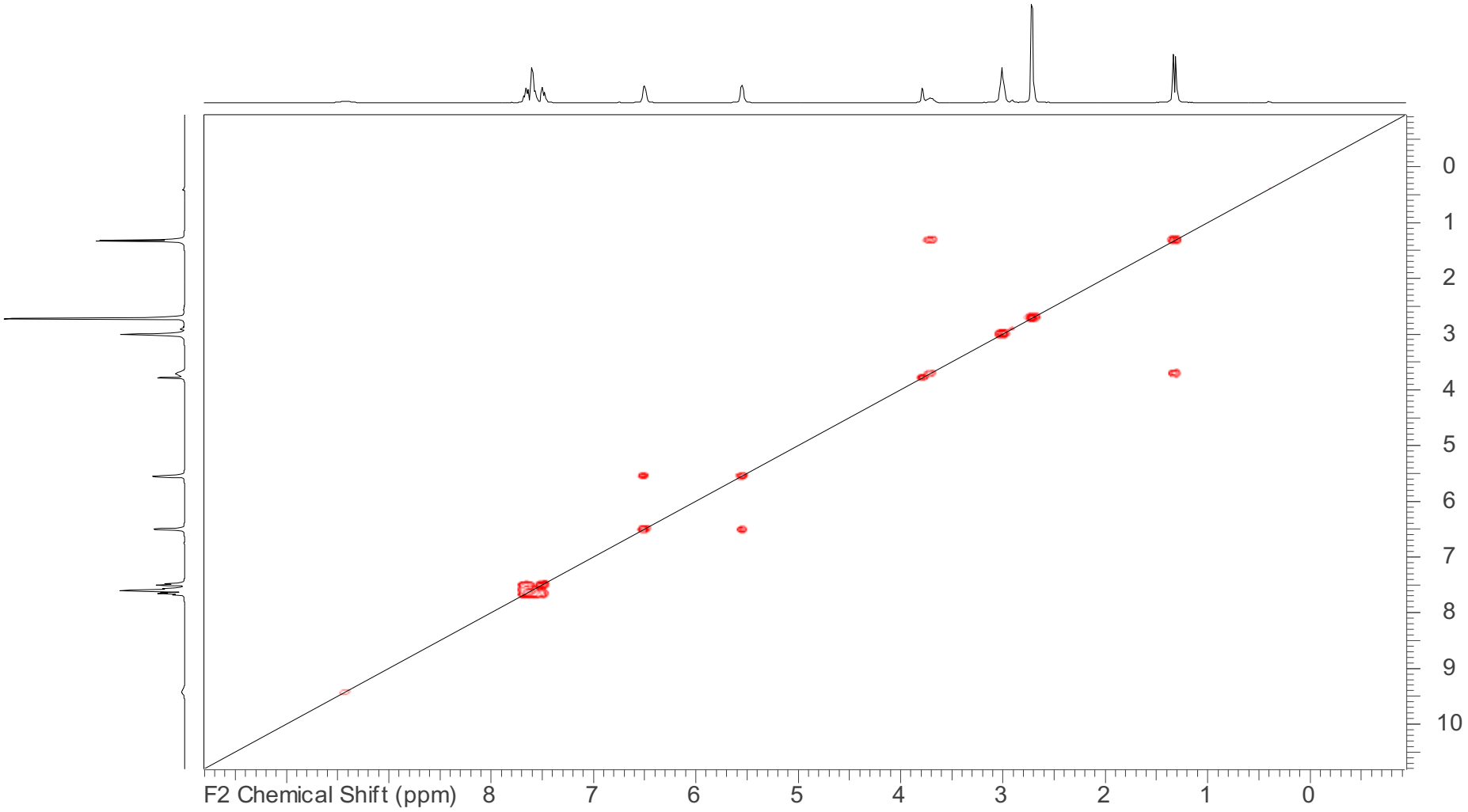

Figure 20 The ^{1}H -^{1}H COSY of **5**. In d_6-DMSO

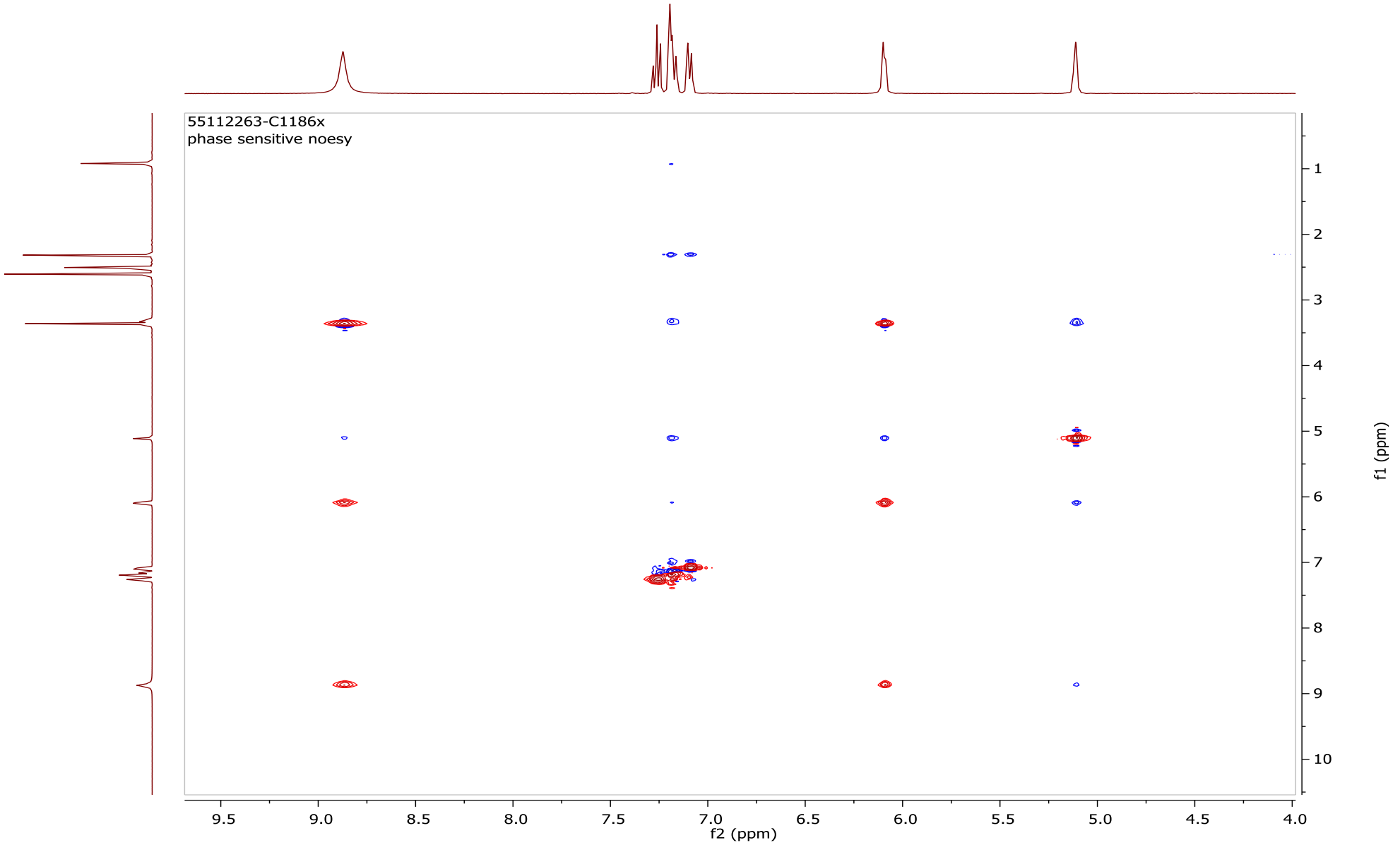

Figure 21 The ^{1}H -^{1}H NOESY of **5**. In d_6-DMSO

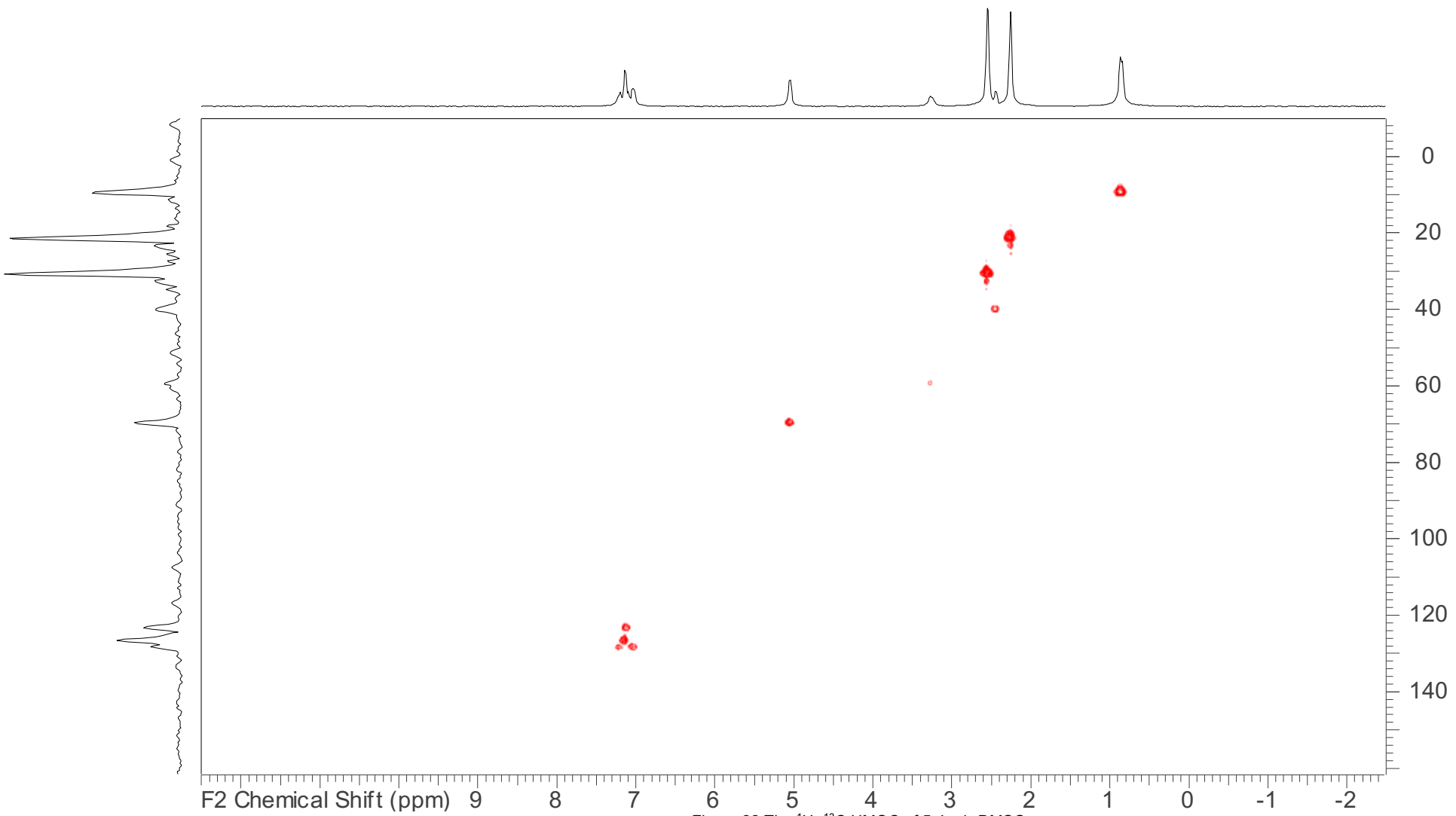

Figure 22 The ^{1}H -^{13}C HMQC of **5**. In d_6-DMSO

8.3. NMR of 4-methylephedrine

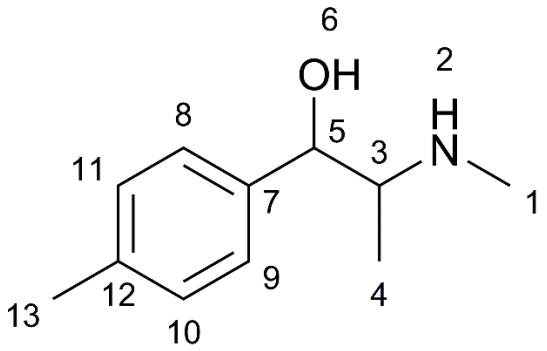

Figure 23 Structure of **6**

Table 5 Summary of ^{1}H and ^{13}C NMR data of **6** in d_6-DMSO

Shift ^{1}H (ppm)	Shift ^{13}C (ppm)	Position	^{1}H NMR Multiplicity	*J*-Value (Hz)
9.01	-	2	br s	-
7.27	129.27	8 10	d	7.33
7.18	126.22	9 11	d	7.33
6.07	-	6	br s	-
5.14	69.7	5	s	-
3.28	59.69	3	s	-
2.60	30.86	4	s	-
2.29	21.24	13	s	-
0.92	9.59	1	d	6.70
-	136.78	7	s	-
-	138.74	12	s	-

On inspection of the ^{1}H NMR spectrum of **6** a doublet of doublets at 7.27 and 7.18 ppm are observed, which arise from the 1,4-disubstituted benzene ring. The pattern of these peaks corresponds with that seen in compound **3**,[28] which has peaks at 7.93 and 7.41 ppm[1] and this is expected as both are 1,4 disubstituted systems. Furthermore, this observation was anticipated as this part of the molecule is independent of the reduction reaction. The symmetry of this section of the molecule is shown with the $^{3}J_{HH}$ coupling constants, which are the same for both peaks 7.33 Hz and shows second order effects. This frequency is consistent with the 6-10 Hz expected for a $^{3}J_{HH}$ on a benzene ring.

Further ^{1}H signals are observed in the ^{1}H NMR spectrum compared to 4-methylmethcathinone. One of these is the peak at 6.04 ppm which corresponds to the additional hydrogen at position (6). A cross peak interaction of this peak does not occur in the ^{1}H–^{13}C HMQC, which is an indication that this is peak is the OH proton. Also in the ^{1}H NMR spectrum, the signal was broad suggesting oxygen is present and is seen for the other compounds. Further evidence is found in the ^{1}H–^{1}H COSY spectrum, in which this proton couples to the proton at position at 5.14 ppm (CH). This coupling would not be realised for the NH_2 protons. Consequently, after consultation of the ^{1}H–^{13}C HMQC the only other peak without a carbon is 9.01 ppm; this peak is the NH_2 protons as the peak area has an integral of two protons by ^{1}H NMR.

The integration of the peaks revealed that the peak at 2.60, 2.29 and 0.91 ppm were the equivalent of three protons and this is suggestive that each peak is a methyl group. The ^{1}H NMR signal at 0.91 ppm is a doublet which is consistent with the environment of the (4) position protons with the doublet arising from the one adjacent ^{1}H. This was further evidenced with the ^{1}H–^{1}H COSY, which demonstrated

coupling with the proton at 3.28 ppm. Looking at the ^{1}H–^{1}H COSY the peak at 2.29 ppm connects to the aromatics at 7.18 ppm. This, therefore, shows that this methyl group must be the protons at position (4). The final peak at 2.60 ppm by elimination must be the N-CH_3. The ^{1}H– ^{1}H COSY shows no correlation between this peak and the rest of the compound demonstrating the isolation from other proton environments.

The ^{1}H– ^{13}C HMQC allowed for the easy assignment of the ^{13}C NMR spectrum as this allowed the pre-assigned ^{1}H NMR spectrum to be used to assign each peak. This allowed all but two peaks to be assigned; the peaks at 137.2 ppm and 139.21 ppm. These two peaks, by the fact they did not appear in the HMQC, suggests that they have no hydrogens attached to them. This narrowed it down to carbons (7) and (12), which are quaternary carbons. The peak at 139.21 ppm corresponds to the carbon at position (7) as it is closer to the OH group, which is electron withdrawing, and hence has less shielding than the other carbon of interest.

After inspecting the Fourier Transform Infra-Red (FTIR) spectrum of **6**, (see section 3.7) a link between the NH_2 and the OH was seen as a deformation of the OH peak. To explore this anomaly, a ^{1}H-^{1}H NOESY (Figure 26) was conducted to explore the possibility of an exchange between the two electronegative groups. The peaks show a Nuclear Overhauser Effect (NOE) effect through space from the aromatic peaks at 7.18 ppm to the peak at 0.91 ppm showing that these two environments are close together and can interact. This confirms what was seen in the ^{1}H-^{1}H COSY with the 0.91 ppm peak resonating with the proton at position (3). A further exchange signal connects the peaks at 6.02 and 9.01 ppm; this demonstrates that an exchange process was happening between the nitrogen hydrogens (2) and the hydroxyl group (6).

Comparing **6** to the analogous methylmethcathinone (**3**), the differences arise from the addition of a proton on position (5), seen as the peak at 5.1 ppm, and the reduction of the carbonyl group to alcohol which gives rise to the peak at 6.1 ppm. The original peak at 5.1 ppm has shifted downfield due to the de-shielding effects from the electronegative OH. The other difference is in the ^{1}H-^{1}H NOESY where the alcohol exchanges with the amine. This does not occur in the **1** - **3**, which could be due to the lack of protons on the carbonyl. When comparing the rest of the spectrum, the aromatic region matches along with the other peaks.

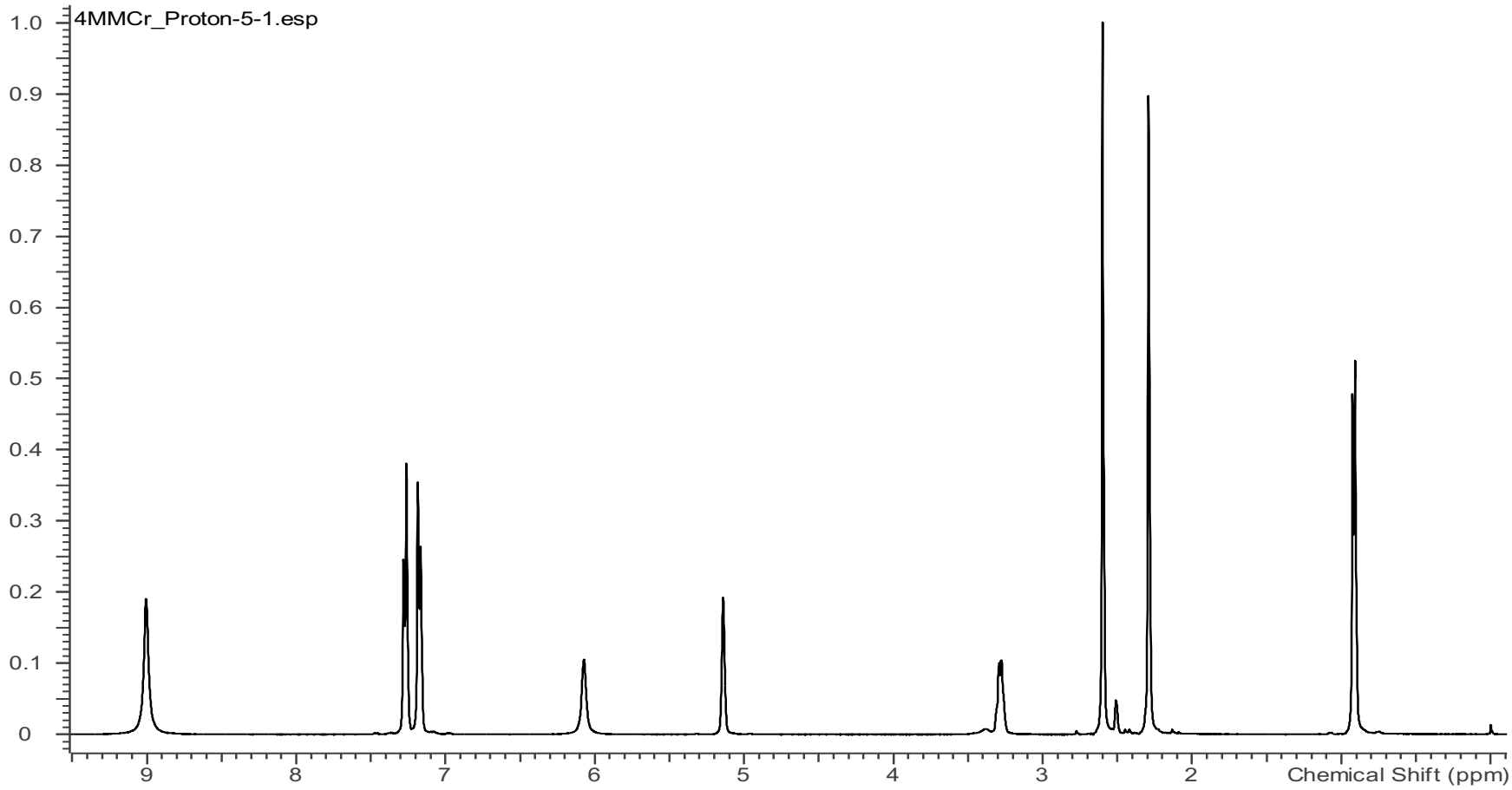

Figure 24 ^{1}H spectrum of compound **6** in d_6-DMSO.

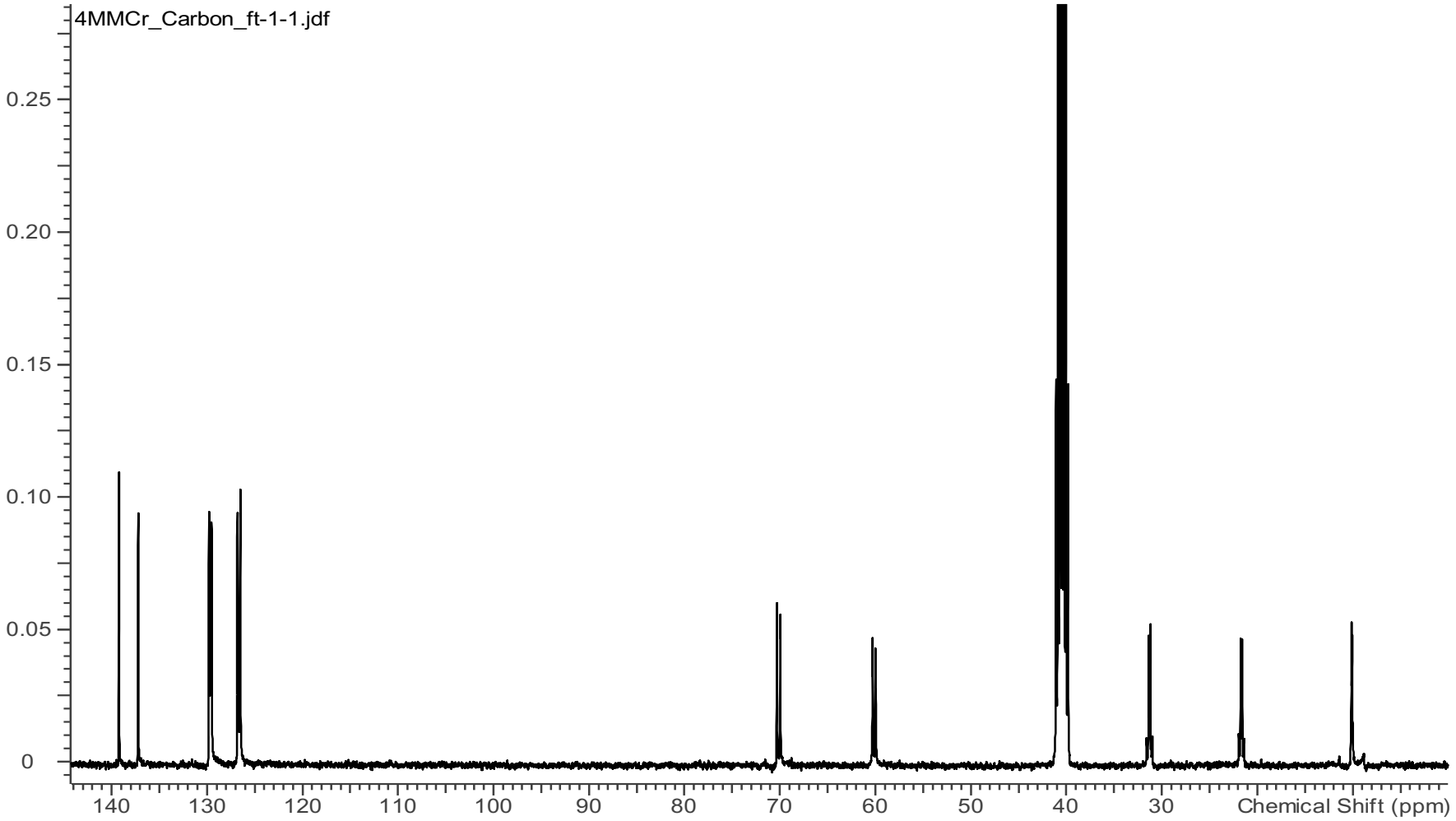

Figure 25 ^{13}C spectrum of compound **6** in d_6-DMSO

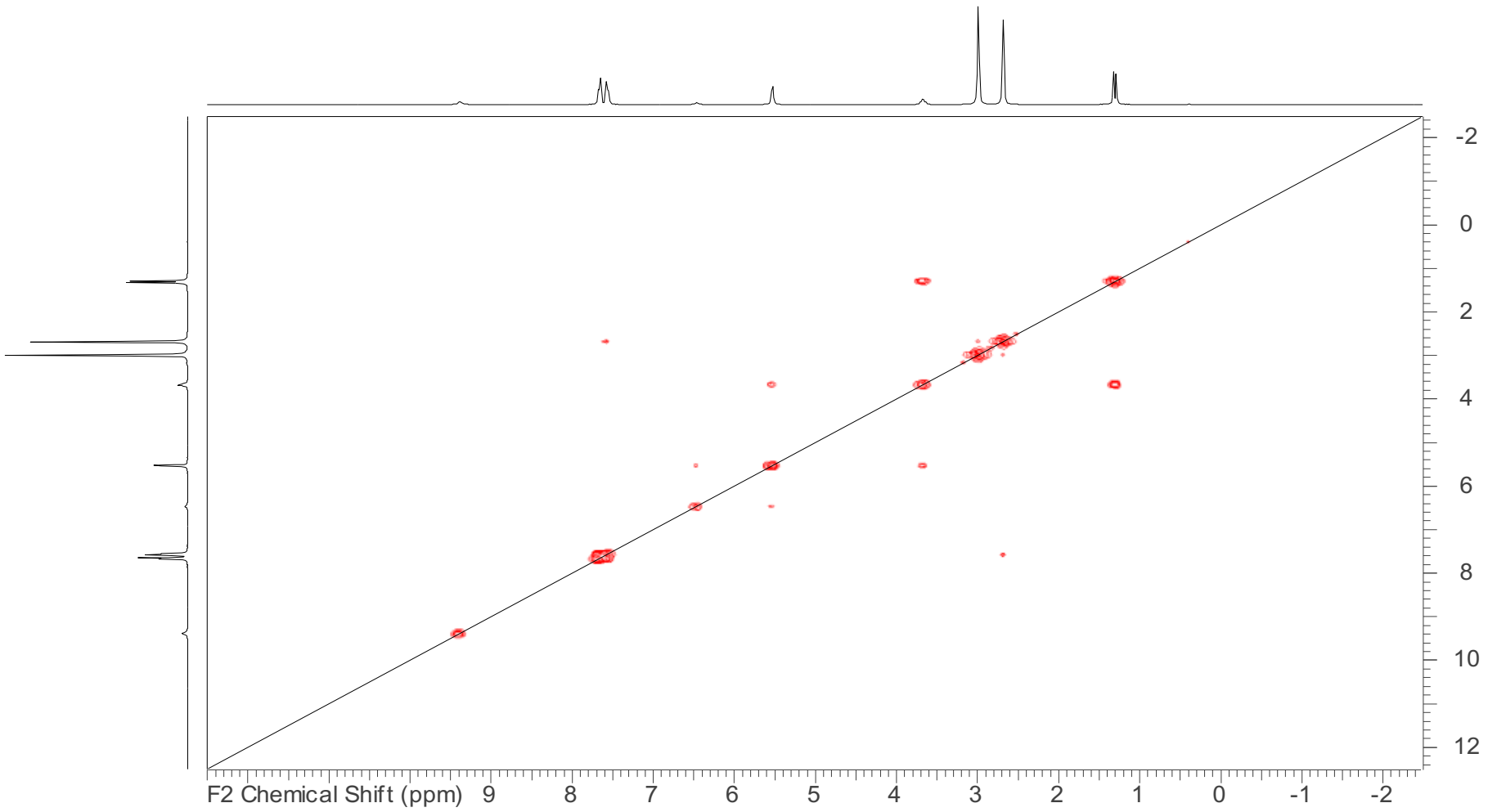

Figure 26 ^{1}H-^{1}H COSY spectrum for **6** in d_6-DMSO.

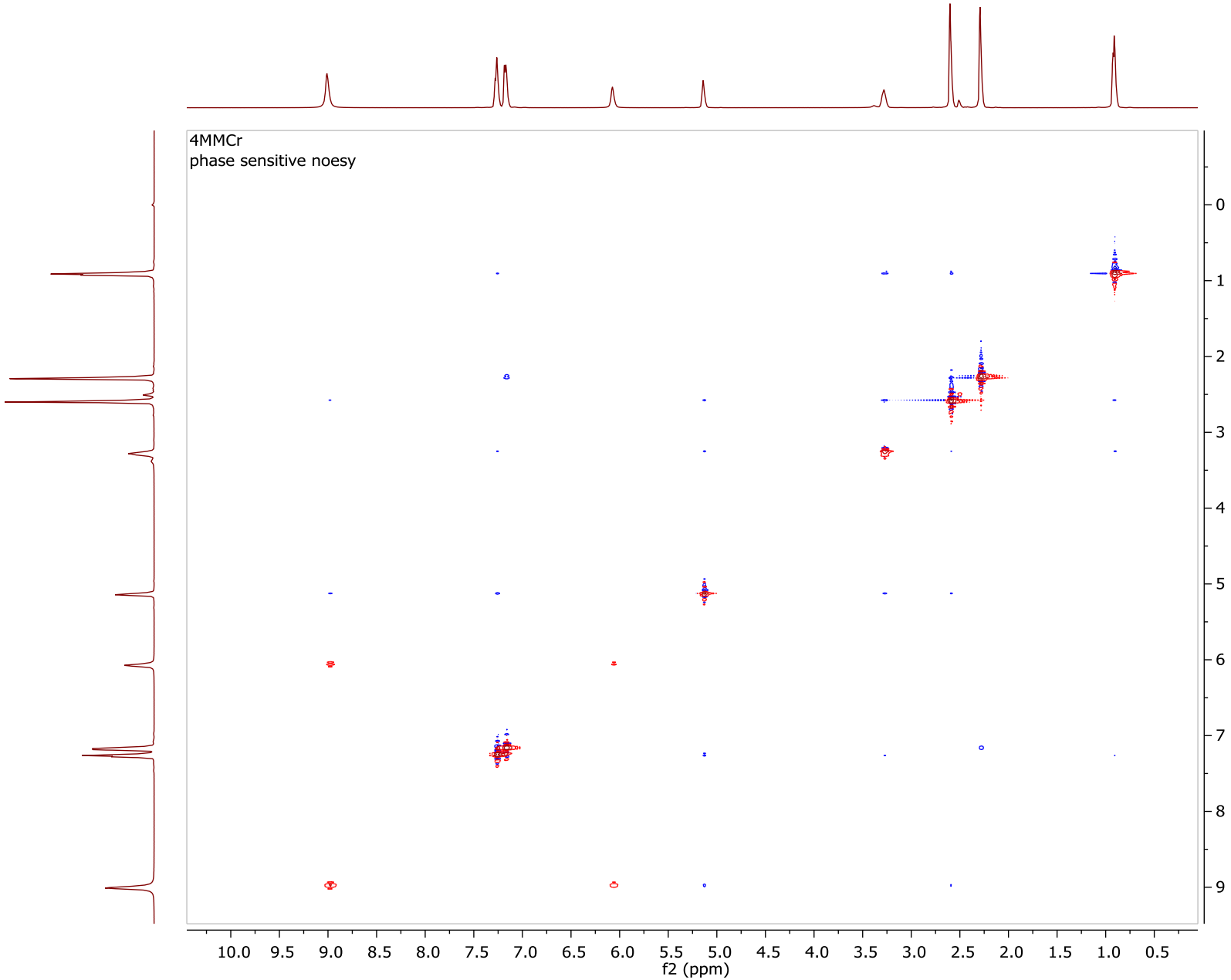

Figure 27 ^{1}H-^{1}H NOESY spectrum for **6** in d_6-DMSO

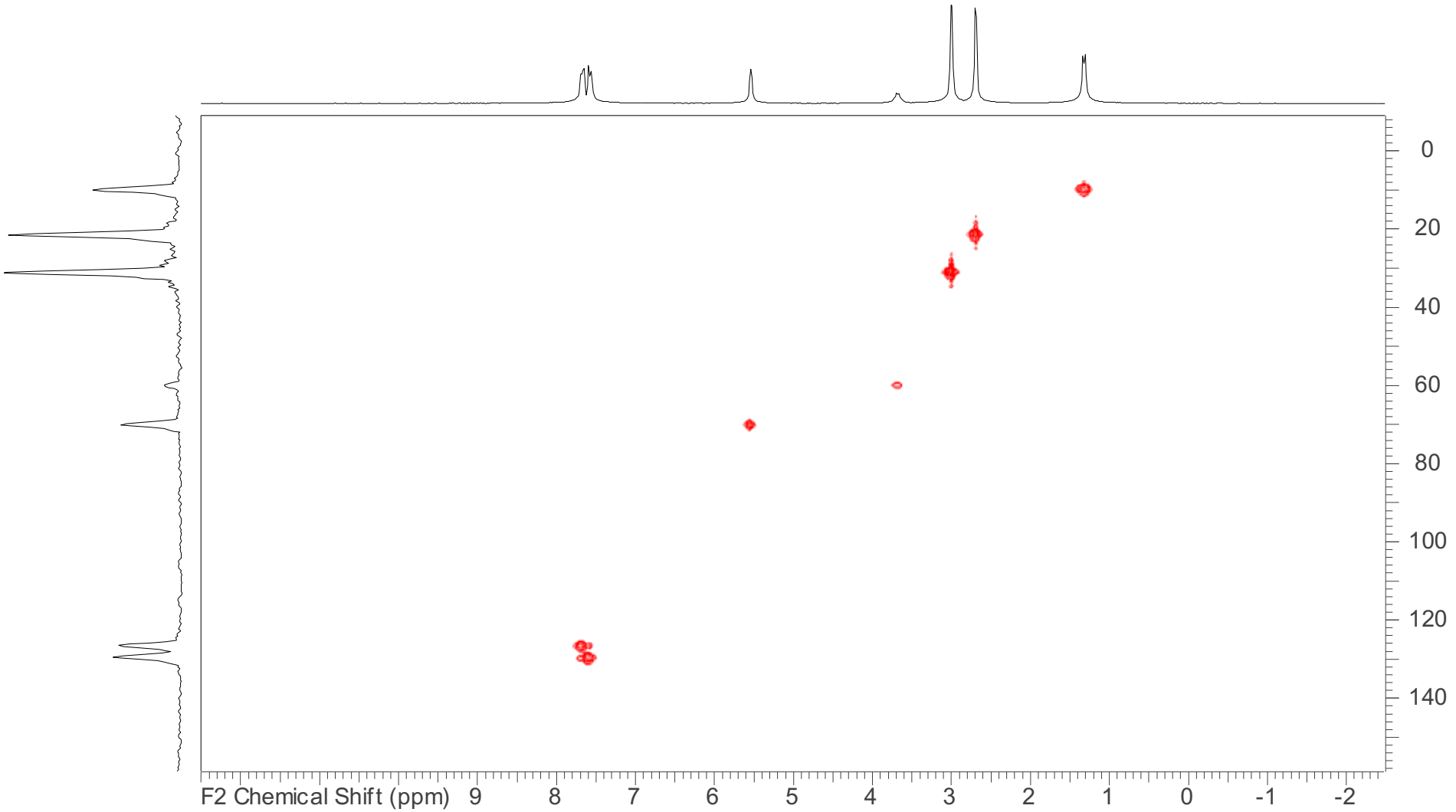

Figure 28 The ^{1}H -^{13}C HMQC of **6**. In d_6-DMSO

8.4. Mass Spectra of methylephedrine Isomers

The mass observed from the LC-HRMS for all three isomers for methylephedrine are within a 10 ppm tolerance at the calculated mass, which allows for a high percentage of accuracy that the proposed structure(s) for the compounds are correct when considered alongside evidence from the NMR studies (although regioisomers cannot be differentiated using this technique).

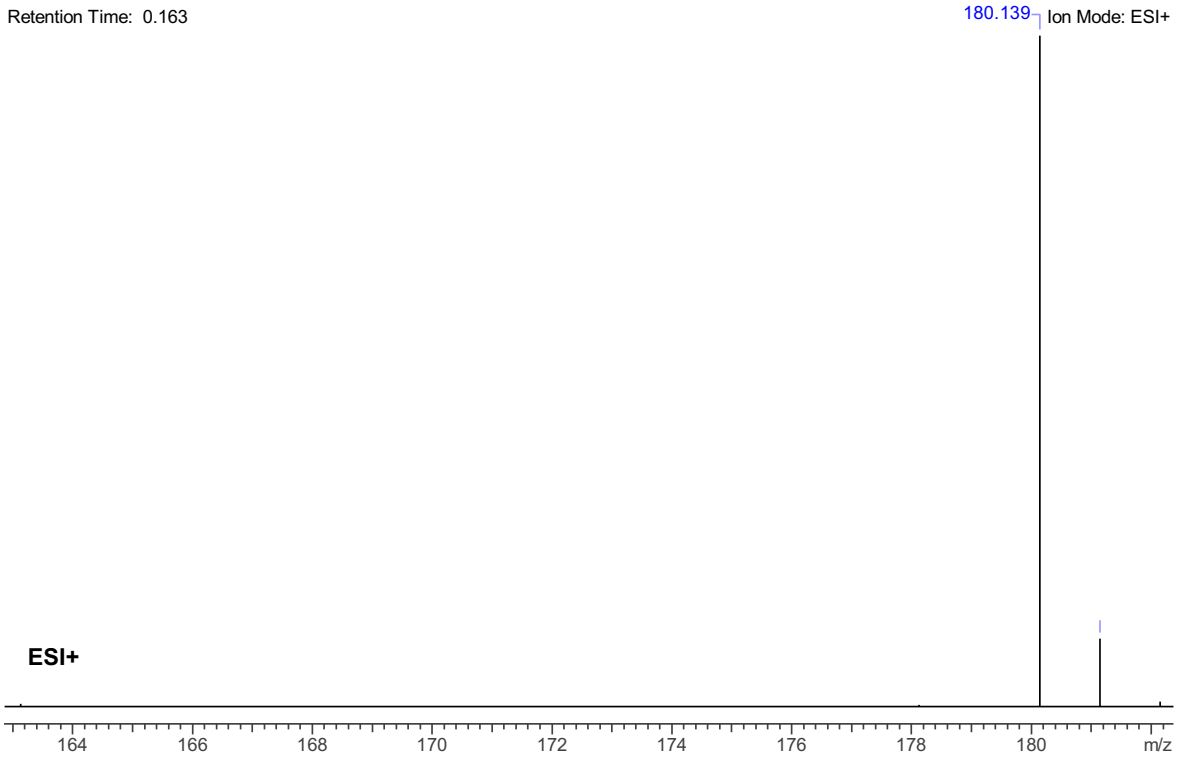

Figure 29 The HRMS of **4** run with loop in Methanol

The fragmentation of **3** and **6** are reported in

Table 6, however, the other regioisomers are analogous to those reported. This data was obtained from EI ionisation (70 eV) from GC-MS. The compounds were not derivatised or altered in any way before running the GC-MS. There are many similarities in the pattern observed. For example, all three isomers exhibit a base peak (m/z = 58) which corresponds to the fragment formed by breaking the bond between the β and α carbon. The fact that this is the base peak shows that it is most stable fragment that forms, under EI, and that this bond is the easiest to break. This would be due to the two highly electronegative centres on either side of the bond drawing electron density away leaving it vulnerable to cleavage by the e^-. The next peak is the one at m/z = 91, which corresponds to the free radical formed by the loss of the aromatic ring. This is again common to both parent and metabolite and all regioisomers. The next ion is the one at m/z = 119 C_7H_6O, which is the other half of the 58 m/z mass fragment C_3H_7N.[29] This is a straightforward loss for methylmethcathinone but for methylephedrine this involves a rearrangement to achieve this fragment. The proposed mechanism is shown in

Figure 30.

Figure 30 Proposed fragmentation mechanism for **6** base peak forming the mass of 58 m/z **4** and **5** are analogous to this mechanism.

Table 6 The major mass fragments from both **3** and **6**. **1**, **2**, **4** and **5** are all analogous. The data is taken from the GCMS spectrum.[47]

Mass (m/z)	Formula	Structure
180	$C_{11}H_{18}NO$	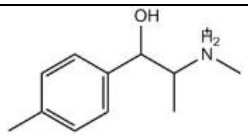
178	$C_{11}H_{18}NO$	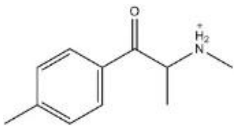
146	$C_{10}H_{12}N$	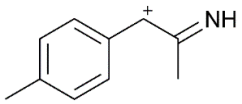
119	C_8H_7O	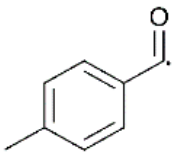
91	C_7H_7	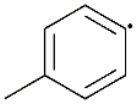
58	C_3H_8N	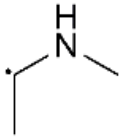

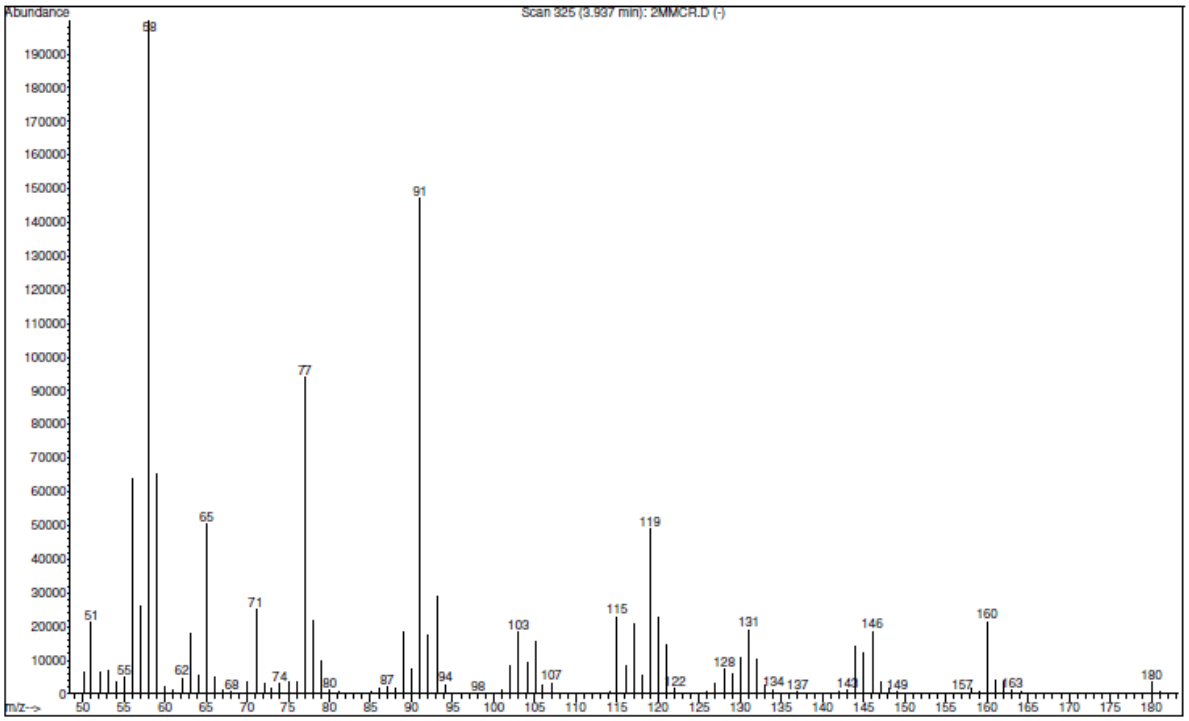

Figure 31 The EI Mass Spectrum of **4** in methanol (2 mg mL^{-1}) with compounds **5** and **6** analogous.

8.5. Ultra-Violet Visible Spectroscopy (UV-VIS) of methylmethcathinones and methylephedrine Isomers

The UV-Vis spectra for **4**, **5** and **6** were observed to be similar with absorbances recorded in the 210, 260 and 270 nm regions (see Table 7). These peaks all have slight variations of about 3 nm. The 272 nm wavelength would refer to a substituted benzene ring. This would be the due to the π→π* transmissions. The absorbance at 215 nm is likely to be a secondary absorbance due to the π-system.

Table 7 Tabulated results for compounds **4**, **5** and **6** in methanol between 200 and 400 nm.

Compound	Concentration	Wavelength (nm)	Absorbance (AU)
4	0.019	210	0.67
		262	1.32×10^{-2}
		397	2.71×10^{-3}
5	0.02	211	0.71
		265	1.78×10^{-2}
		272	1.57×10^{-2}
6	0.2	212	0.65
		263	9.70×10^{-3}
		272	6.43×10^{-3}

When the mobile phase, 5 mM aqueous ammonium formate - acetonitrile [10:90% v/v], is used instead of MeOH as the solvent, there are noticeable changes in the spectra. The first change to note is the shift of the 210 - 212 nm peaks to 211 - 213 nm with **4** and **5** having the same absorbance displaying a bathochromic shift. The peak at 264 nm has remained largely the same. This is most likely to occur because the buffer is forming hydrogen bonds with the auxochromes OH and NH_2, but also charged salt interactions hence altering the wavelength seen.

The work done by Santali *et al* [4] collaborates this as **3** was performed in both HCl (0.1 M) and sodium hydroxide (0.1 M). These solutions displayed a bathochromic shift and hypochromic shift respectively.

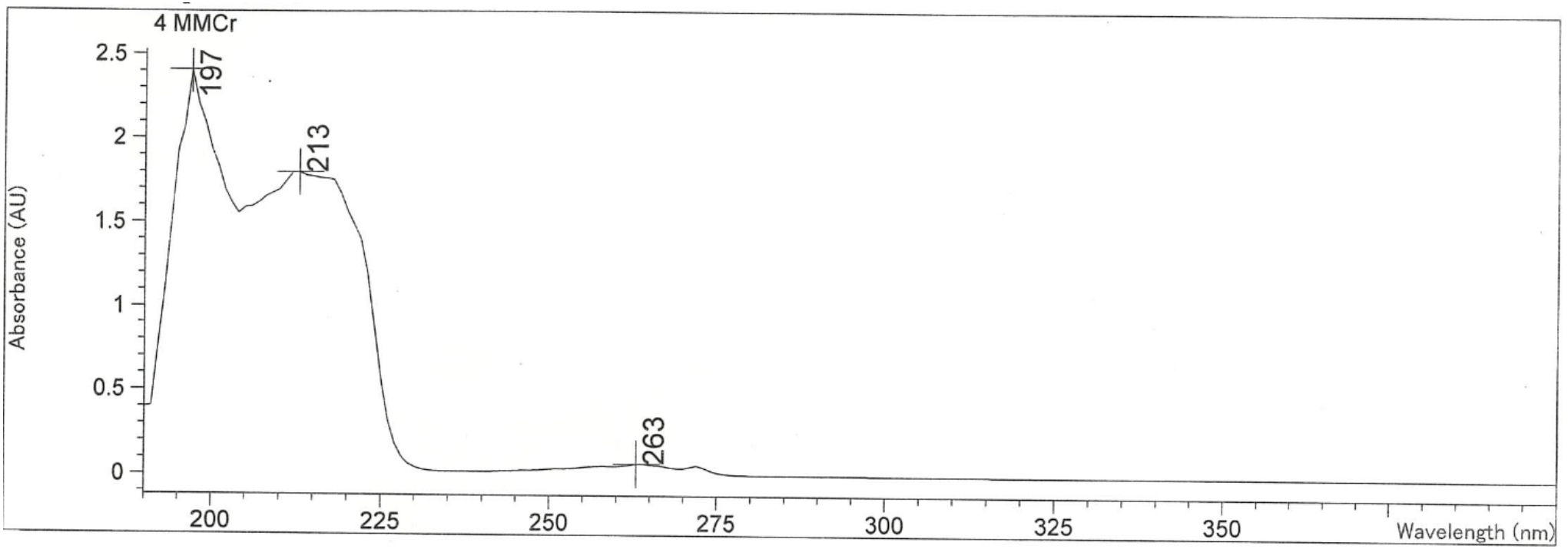

Figure 32: The UV-VIS spectrum of **4** in mobile phase 90:10 MeCN to water (25 µg mL^{-1}).

8.6. Presumptive tests of methylmethcathinones and methylephedrine isomers

Table 8 shows the reactions of methylmethcathinone and methylephedrine with a selection of presumptive test solutions. Chen-Kao is a specific test for ephedrines and Robadope is a test for primary amines,[43] which both methylmethcathinone and methylephedrine do not possess. For the Robadope test, compounds **1**-**6** should give a postive result. However, methylmethcathinone should react with Liebermann's and Zimmermann's.[42, 44]

The results show discrepancies between the published results [42-44] and that of the results presented herein. The results were either negative instead of positive or produced variations in colour. Further investigation into the literature revealed that some researchers used powders directly instead of making a solution.[44] A comparison was tried in order to highlight any differences.

Table 8 The results of the presumptive tests comparing powder to solution 10 μg mL^{-1} showing both initial colour and colour 5 minutes later.

Sample	Liebermans		Robadope		Chen Kao		Zimmermanns		Simons	
	Initial	5 minutes later	Initial	5 minutes later	Initial	5 minutes later	Initial	5 minutes later	Initial	5 minutes later
Blank	-	-	-	-	-	-	-	-	-	-
1 Solution	-	-	-	-	-	+ YELLOW	-	+ PEACH	+ PURPLE	+ PURPLE
1 Powder	-	-	-	-	-	-	-	+ PINK	-	-
4 Solution	-	-	-	-	+ PURPLE	-	-	-	-	-
4 Powder	+ ORANGE	+ DARK YELLOW	-	-	-	-	-	-	-	-
2 Solution	-	-	-	-	-	-	-	-	+ RED	-
2 Powder	+ PALE ORANGE	+ PALE YELLOW	-	-	-	-	-	-	-	-
5 Solution	-	-	-	-	+ PURPLE	-	-	-	-	-
5 Powder	+ ORANGE	+ DARK YELLOW	-	-	-	-	-	-	-	-
3 Solution	-	-	-	-	-	-	-	+ PINK	+ PALE PEACH	+PEACH
3 Powder	+PALE ORANGE	+ PALE YELLOW	-	-	-	+ GREEN	-	-	-	+ DARK PEACH
6 Solution	-	-	-	-	+PURPLE	+PALE BLUE	-	-	-	-
6 Powder	+ DARK ORANGE	+ PALE ORANGE	-	-	-	+ BLUE WITH GREEN MOTTLE	-	-	-	-

The results in Table 8 show a slight differentiation between a solution or a powder, which can lead to false negatives in some cases. For example, looking at **6** it is supposed to react with Chen-Kao reagent. However, this seems to be the case only for the sample in a solution and not as a powder. This pattern is also seen in with **4** and **5**. The proposed complex formed in the Chen-Kao test can be seen in Figure 33, which is the formation of a copper chelate complex.[48]

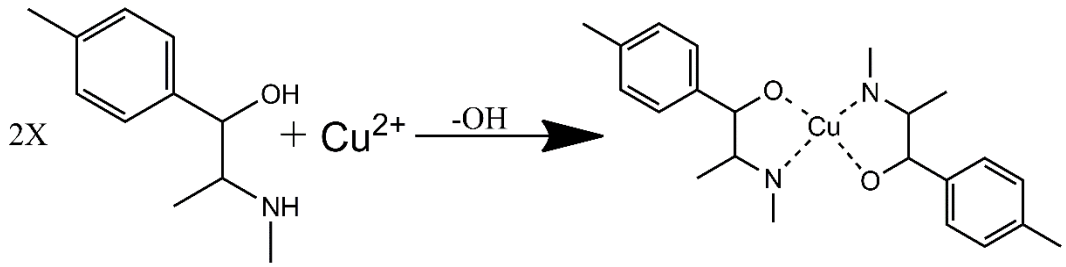

Figure 33 The proposed formation of the Chen Kao complex for methylephedrines[48]

For Liebermann's reagent, the DEA paper on this test for cathinones does not shed any light on the mechanism (or propose a mechanism), however, as it utilises sulphuric acid/sodium nitrite, it is possible that the mixture is forming a highly coloured *N*-nitroso derivative.[49] This test has been shown to work with cathinones and its derivatives before by Toole *et al.*[44] The mechanism could follow that proposed and depicted in Figure 34 with sulphuric acid facilitating the dehydration of the nitrite. Compounds **4**–**6** attack the positive $^{+}$N=O forming the corresponding coloured *N*-nitroso derivative.[49]

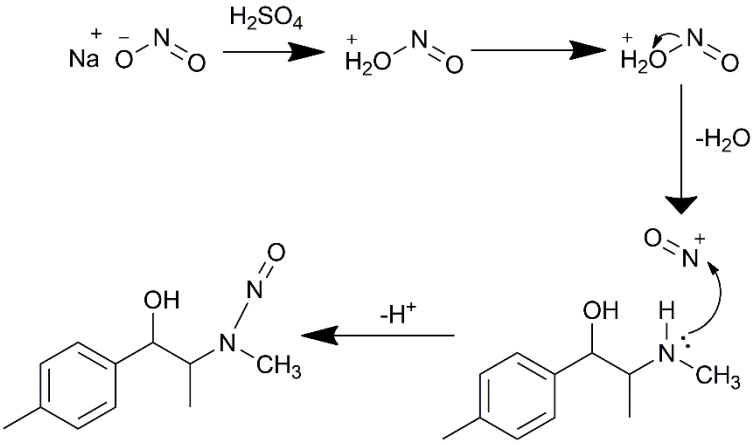

Figure 34 The proposed mechanism of forming a coloured N-nitroso derivative of the ephedrine(s)[44]

Robadope and Simons are the tests for primary and secondary amines respectively, so looking at the structures this means that the samples should only react with Simons as they are secondary amines. The difference between the two is the use of acetone in Robadope and acetaldehyde in Simons. This gives rise to a complex with a -4 charge over one with a -3 charge.[48] This comes from the additional hydrogen in the iron complex (Figure 35). The mechanism for the formation of these molecules is *via* the formation of an enamine, which then reacts with the nitroprusside. This is then hydrolysed to the Simon-Awe complex. The Simon-Awe complex will then react with a secondary amine, however, with ephedrine type compounds the presence of the electronegative hydroxyl group nearby disrupts the reaction.[50] The Robadope reagent follows the same process.

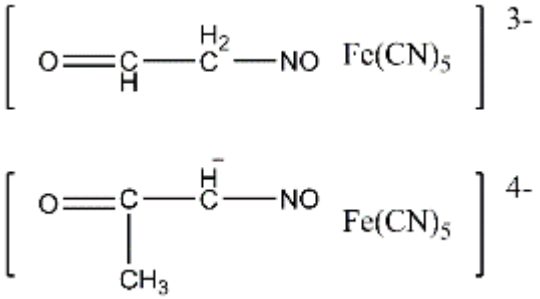

Figure 35 two key molecules in the Simons and Robadope presumptive tests. Top Simons. Bottom Robadope.[48]

The selection of the Zimmermann's reagent is recommended by UNODC as a presumptive test for synthetic cathinones.[42] Although Table 8 shows no immediate reaction with the reagent, the colour change did take place within 5 minutes of the solution being added and, as can be seen in Table 8, gave rise to a purple/pink colour. This is different from what is reported by Nic Deiad *et al*.,[51] who reported an initial colour change to purple. The Zimmermann's reagent works through the formation of a Meisenheimer complex.[52] This is achieved in alkaline conditions where the dinitrobenzene reacts with the β carbon. The final complex is shown in Figure 36. The difference in the reported results and those reported here is not readily explained but is likely to be the slow oxidation of the Meisenheimer complex to form the final coloured product.

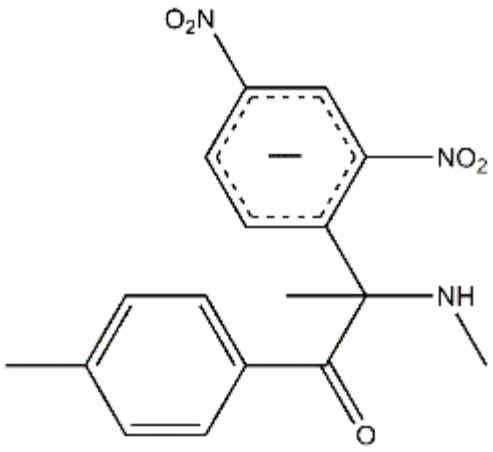

Figure 36 Proposed structure of the complex formed with Zimmerman's reagents showing compound **3**, however, **1** and **2** are analogous.[52]

8.7. Fourier Transform Infra-Red Spectroscopy

The first difference to note between **1**-**3** and **4**-**6** is the addition of the O-H stretch at 3306, 3292 and 3349 cm^{-1} respectively for compounds **4**-**6** (see Figure 37), which is absent for **1**-**3**. However, this peak lacks its normal broad appearance. From this, it was expected that having another polar group like the amine nearby would affect this IR band (see NOESY data in section 8.1, 8.2 for evidence of this interaction). The other notable difference is the loss of the band at 1694, 1687 and 1686 cm^{-1} for compounds **1**, **2** and **3** respectively. These bands for the methylmethcathinone regioisomers corresponds to that seen in the other literature by Power *et al.*[1] This band corresponds with the carbonyl in **1** - **3**, however, following the reduction of the carbonyl, this band is lost. The difference of **1**'s higher band of 1696 cm^{-1} is due to steric effects of the methyl component on the aromatic ring.[1] The out of plane C-H bending bands of **4**-**6** are as follows; 752 cm^{-1} for **4**, the bands at 892, 752 and 720 cm^{-1} for **5** and the band at 827 cm^{-1} for **6** match those seen in the respective regioisomers of methylmethcathinone.[1]

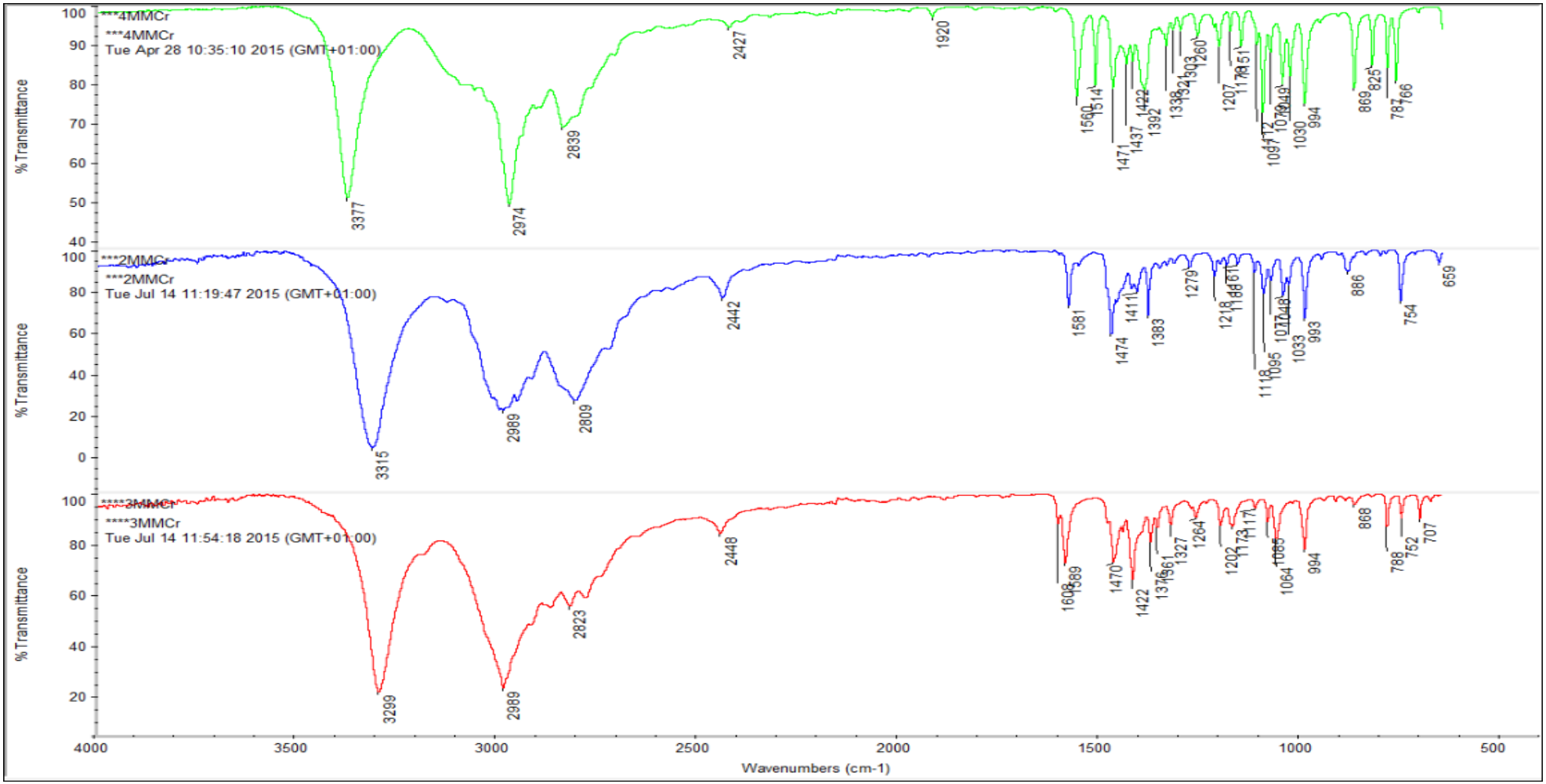

Figure 37 The FTIR-ATR spectra for compounds **4**, **5** and **6**. Spectra have been processed for ATR correction.

8.8. HPLC-UV Method Development

The HILIC method developed by Khurana[45] was the starting point for the separation of the methylmethcathinone and the methylephedrine regioisomers using HPLC-UV in the HILIC mode. The method used an ACE-SIL 5 (150 x 4.6 mm 5 μm) column, a mobile phase of 5 mM aqueous ammonium formate - acetonitrile [10:90% v/v], a flow rate of 1 mL min^{-1}, and a detector wavelength of 264 nm. The method was adapted by adding a separate wavelength of 215 nm for **4** - **6**. This was due to the results of the UV spectra in section 0 demonstrating that the 215 nm peak has the greatest intensity. The order of elution was observed to be compounds **1** (t_R = 7.38), **2** (t_R = 7.95) and then **3** (t_R = 8.60). The method achieved a resolution > 2 required by the ICH guidance[46] as the separation between **1** and **2** was 2.11 and between **2** and **3** was 2.25. This method also showed excellent symmetry of 1.05, 1.01 and 1.00 for **1**, **2** and **3** respectively. The results of this method being applied to compounds **4**-**6** show a resolution of 0.98 between compounds **4** and **5**. This small resolution is not enough to confidently integrate areas and have reliable data. The order of elution was **4**, **5** and then **6**.

The method was modified by varying the flow rate and the column temperature. The Flow Rate (FR) varied from 0.8 mL min^{-1} to 1.3 mL min^{-1}. The data shown in Table 9 shows that even though the retention times change the resolution remains the same. The resolution was calculated using

Equation 1, which uses the width at half peak maximum. The lack of change in the resolution demonstrates that the mechanism for this method is not dependant on the flow rate of the mobile phase and the analytes within it. The pK_a of the metabolites (**4**-**6**) was calculated to be 9.3 and for the parent (methylmethcathinone) to be 7.9. These values are theoretical and calculated through Chemdraw. The data

could potentially indicate that the more polar layers formed by the HILIC method is in this instance less likely to be influenced by the change of flow rate.

$$Resolution = \frac{1.18(t_{R1} - t_{R2})}{w_1 - w_2}$$

Equation 1 equation for the calculation of resolution in Agilent ChemStation.

Table 9 Tabulated data showing the retention times and resolutions with variation in flow rate for **4** – **6**. temperature = 22°C, Mobile phase 5 mM aqueous ammonium formate - acetonitrile [5:95% v/v].

Compound	Flow rate (mL	t_R	Resolution
4	0.8	9.27	-
5	0.8	9.50	0.93
6	0.8	9.73	1.04
4	1	7.56	-
5	1	7.64	0.99
6	1	7.83	0.99
4	1.3	5.03	-
5	1.3	5.60	1.02
6	1.3	5.90	1.03

The next parameter to be altered to increase the resolution was the column temperature. Originally run at 22°C the method was altered to run at 30°C. Table 10 shows the results of this change. The resolution slightly increased, however, the retention time had increased. The higher temperature would allow for lower operating pressures. A potential reason why the retention time has shifted could be due to the mobile phase being less viscous, therefore allowing the solvent to defuse through the column more quickly, thus changing the retention time of the analytes, and effecting the resolution.

Table 10 Tabulated data from the 30°C and 22°C runs of 5 mM aqueous ammonium formate - acetonitrile [5:95% v/v]. FR = 1 ml min^{-1}

Compound	Temperature (°C)	t_R (minutes)	Resolution
4	30	23.07	-
4	22	19.08	-
5	30	24.03	0.98
5	22	37.24	1.55
6	30	24.97	0.85
6	22	38.80	1.65

As the previous variations in temperature and flow rate had failed to alter the resolution enough and hence the separation mechanism, the next step was the altering of the ionic strength of the mobile phase. This was achieved by increasing the concentration of ammonium formate from 5 mM to 20 mM. This was not increased further as this method may be transferred onto a LC-HRMS. Therefore, the concentration of buffer could not exceed 20 mM or the LC-HRMS Electrospray Ionisation (ESI) source would not be able to dry and create gaseous ions, which high ionic strength buffers inhibit. The method was altered to run with 20 mM (Table 11); however, there was no significant change in the resolution. This means that either the analyte has been fully ionised so that the mechanism is unaffected by increasing the polarity of the mobile phase. This would mean that this separation is being driven by the hydrophilic partitioning or hydrogen bonding as neither of these would be influenced by the charging of the analyte.

Table 11 The results of increasing the buffer concentration showing retention times and resolution for methylephedrine regioisomers temperature = 22°C, Mobile phase 20 mM aqueous ammonium formate - acetonitrile [5:95% v/v].FR = 1 ml min^{-1}.

Compound	Buffer	t_R (minutes)	Resolution
4	20	13.48	-
4	5	23.06	-
5	20	13.97	1.13
5	5	24.04	0.98
6	20	14.50	1.18
6	5	24.97	0.85

The column was changed to determine if a longer column and smaller particle size would increase the resolution. The effect of changing the column length and particle size on resolution can be seen by the change of efficiency between the columns. The efficiency was calculated by

where l is the column length and d_p is the particle size. The equation gave an efficiency of 15 for the 150 x 4.6 mm 5 µm column, but the 250 x 4.6 mm 3 µm column gave an efficiency of 42. As a result, the column length was increased to 250 mm and the particle size reduced to 3 µm.

$$N = \frac{l}{2d_p}$$

Equation 2 The equation used to calculate the theoretical column efficiency[53]

In fact the running of a longer column had an adverse effect, in that it caused **4** and **5** to co-elute. However, the resolution between the *para*-regioisomer and the *meta*- and *ortho*-regioisomers is improved compared to the shorter column. This could be due to the analytes being suspended within the column longer than with a shorter

column.

Finally, the mobile phase ratio was adjusted. The aqueous content was decreased and the acetonitrile portion was increased, however, the ammonium formate buffer concentration remained constant at 5 mmol and the column used was the 150 x 4.6 mm 5 µm silica. The increase of the mobile phases polarity and hence hydrophobicity had a large effect on the mechanism. All three compounds for (**4**–**6)** co-eluted at 58 minutes or potentially eluted with a t_R greater than an hour, which would not have been detected. This makes this ratio unsuitable as an analytical method. The hydrophilic extraction and hydrogen bonding has potentially forced the analytes to interact greatly with the silica stationary phase and thus resulted in slower movement through the column or even binding of the analytes to the stationary phase. This has been reported for other HILIC methods.[39]

The need to separate the regioisomers did not adversely affect the real world applications of this method due to the unlikeliness of the user taking a *para*-regioisomer and the *meta*-regioisomers being produced *in vivo*. The aqueous content of the method was increased to decrease retention time. The final method had a mobile phase composition of 5 mM aqueous ammonium formate - acetonitrile [10:90% v/v]. The column was the Hichrom Ace-SIL 5 (150 x 4.6 mm 5 µm), with a temperature of 30°C, a flow rate of 1 mL min^{-1} and the wavelengths selected were 215 nm and 264 nm. The auto-sampler was set to inject 20 µL of sample. This method is ready for validation; Figure 38 shows the results of the separation and Table 12 shows the tabulated data for the method.

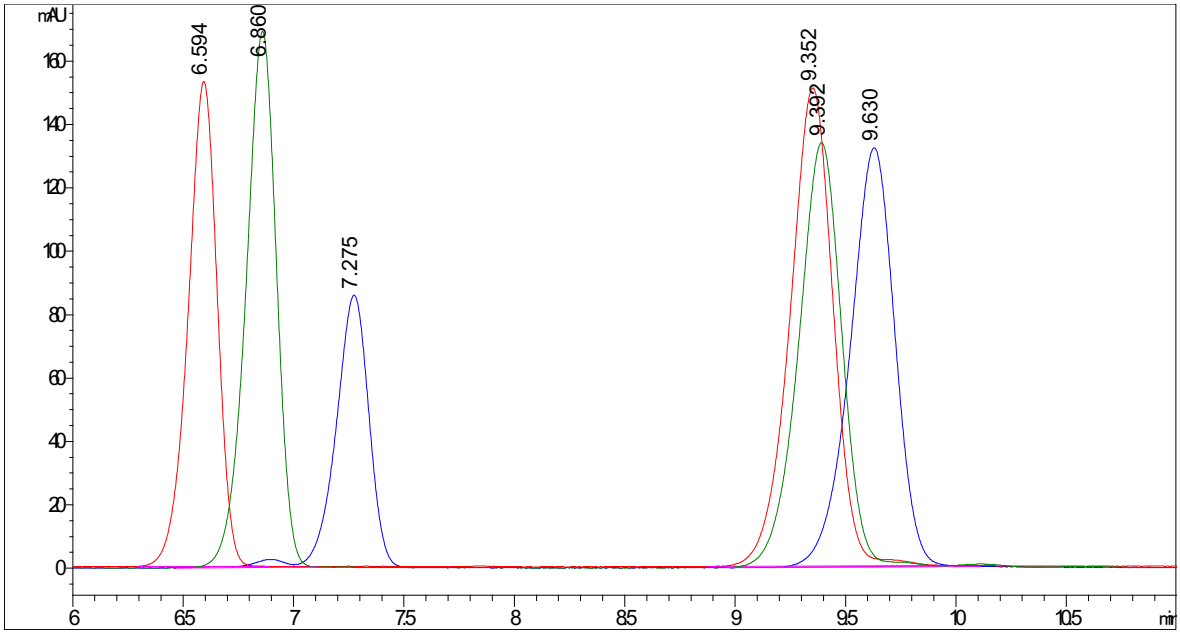

Figure 38 the separation of **1** – **6** with 5 mM aqueous ammonium formate - acetonitrile [10:90% v/v], 150 X 4.6 mm 5 µm column, FR = 1 mL min^{-1}, and a temperature = 30°C. Red = Compounds **1** and **4**, Green = Compounds **2** and **5**, Blue = Compounds **3** and **6.**

Table 12 The results of the final method before validation, with 90:10 acetonitrile:ammonium formate 5 mM, 150 x 4.6 mm 5 µm column, FR = 1 mL min^{-1}, and a temperature = 30°C. a = colour of trace on figure 22.

Compound	Retention time	Resolution	Trace Colour [a]
1	6.59	-	Red
4	9.35	9.29	Red
2	6.86	-	Green
5	9.39	8.90	Green
3	7.28	-	Blue
6	9.63	7.38	Blue

8.9. Validation of the HPLC Method

The validation of the method followed the guidance set out by the ICH.[54] This used linearity, precision, LOD, LOQ, accuracy, selectivity, along with robustness to determine the methods potential.

Linearity was calculated using five calibration standards over the range of 2.5 to 25 µg mL^{-1} for **1**-**3** and a range of 5 to 50 µg mL^{-1} for **4**-**6**. From the five replicate injections the linearity was observed from the plot of concentration versus response for each injection. Linearity was taken from the line of best fit and the R^2 value.

Precision was calculated from the five replicate injections of the calibration standards. This used the %RSD for the areas of each peak. *LOD and LOQ* were calculated as per the guidance given by the ICH.[46] The equations used are shown in Equation 3.

$$LOD = 3.3\frac{standard\ diviation\ of\ the\ response}{slope}$$

$$LOQ = 10\frac{standard\ diviation\ of\ the\ response}{slope}$$

Equation 3 The equations used to calculate the LOD and LOQ[46]

Accuracy looked at the performance of the method at the 80%, 100% and 120% mark of the target concentration of 20 μg ml^{-1} for the regioisomers of methylephedrine and 10 μg ml^{-1} for the regioisomers of methylmethcathinone. This also assessed the %RSD recovery of the compounds from acetonitrile.

The selectivity looked for the potential overlap of other similar compounds which could cause a potential misinterpretation of the results. These similar compounds can come from the synthesis process or even from the interaction within the body. The selectivity used the addition of 4-methylcathinone (7), amphetamine (8), methamphetamine (9) and dihydronormephedrone (10) and these compounds are shown in

Figure 39.

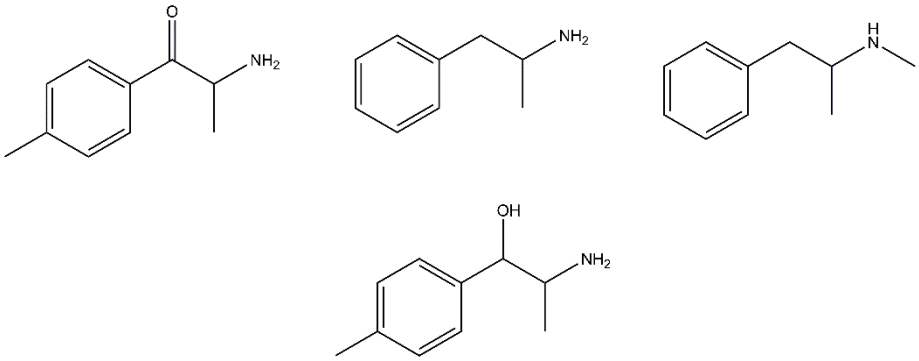

Figure 39 The structure of the analytes used in the selectivity study. Top Left: 4-methylcathinone **7.** Top middle: amphetamine **8**. Top right: methamphetamine **9**. Bottom: dihydronormephedrone[55] **10**

Robustness assessed the changes in flow rate, temperature and mobile phase composition. The flow rate was varied by 0.1 ml min^{-1} above and below the target flow rate. The temperature was varied by 2°C above and below the target temperature of 30ºC. The mobile phase composition was varied by 1% with respect to the aqueous ammonium formate 5 mM percentage.

Table 13 The summary of the validation data of the 5 mM aqueous ammonium formate - acetonitrile [10:90% v/v]. (a) Relative retention time to corresponding regioisomer of methylmethcathinone. (b) Limit of detection using the standard deviation of the response and the slope. (c) Limit of quantification using the standard deviation of the response and the slope. (d) concentrations used for **1** - **3**. (e) The concentrations used for **4** - **6**. (f) the dead volume elution time measure from blank injection using toluene. (g) y = 16.714x - 2.1106 (h) y = 32.21x + 2.3201 (i) y = 48.175x - 2.9072 (j) y = 1.873x + 10.301 (k) y = 35.355x - 9.848 (l) y = 36.021x - 5.0146

	Analytes					
Parameter	1	2	3	4	5	6
t_0 (mins)[f]	0.85					
Rt (mins)	6.62	6.72	7.29	9.39	9.39	9.66
RRT[a](mins)	1.00	1.00	1	1.42	1.39	1.32
Capacity factor (K')	5.62	5.72	6.29	8.39	8.39	8.67
N (plates)	12130	11975	11756	11285	11222	10956
H (m)	$1.24x10^{-5}$	$1.25\ x10^{-5}$	$1.28\ x10^{-5}$	$1.33\ x10^{-5}$	$1.34\ x10^{-5}$	$1.37\ x10^{-5}$
Resolution (R_s)	-	-	-	9.29	8.91	7.38
Symmetry Factor (As)	0.62	1.18	0.62	0.52	1.19	0.52
LOD [b]($\mu g\ ml^{-1}$)	0.07	0.05	0.05	0.28	0.34	0.10
LOQ [c]($\mu g\ ml^{-1}$)	0.21	0.15	0.15	0.84	1.04	0.30
Co-efficient of regression (r^2)	0.9999[g]	0.9999[h]	1[i]	0.9998[j]	0.9998[k]	1[l]
Precision (% RSD) (n = 5)						
50 $\mu g\ ml^{-1}$ [e]	n.d	n.d	n.d	0.13	0.36	0.29
40 $\mu g\ ml^{-1}$ [e]	n.d	n.d	n.d	0.02	0.85	0.14
25 $\mu g\ ml^{-1}$ [d]	0.19	0.17	0.16	n.d	n.d	n.d
20 $\mu g\ ml^{-1}$ [de]	0.16	0.14	0.14	0.22	0.87	0.24
10 $\mu g\ ml^{-1}$ [de]	0.32	0.21	0.27	0.46	0.42	0.76
5 $\mu g\ ml^{-1}$ [de]	0.94	0.38	0.52	0.47	0.33	0.94
2. $\mu g\ ml^{-1}$ [d]	0.86	0.73	0.60	n.d	n.d	n.d

The Height Equivalent Theoretical Plates (HETP) was examined next. This is shown in row N in Table 13; the smaller the number allows for more plates to be compacted into an area (column) therefore increasing the efficiency of the method at separating the compounds. This value is calculated by the division of the length of the column in meters by the number of plates reported by the Equation 4.

$$HETP = \frac{Column\ length\ in\ m}{Plates}$$

Equation 4 equation used to calculate the Height Equivalent Theoretical Plates (HETP)

The Relative Retention Times (RRT) reveal that there are variations between each of the compounds but not enough to separate. The relative retention time will be used to compare the robustness of the method each RRT will be relative to the regioisomer of methylephedrine corresponding regioisomer of methylmethcathinone.

The *Linearity* can be assessed from the line of best fit from the graph of concentration to response. The R^2 value shows the closeness of the data to the line of regression, the data in Table 13 shows that a value greater than 0.9998 was achieved for all compounds. The closeness of this data to the ideal (1) means that it has an excellent linearity.

The *precision* was studied by looking at the percentage relative standard deviation of the areas of each of the five injections shown in Table 13. These data demonstrated a variation of less than 1% in the areas of the calibration standards, which according to the CDER is acceptable.[54]

The *LOD and LOQ* showed a low quantification level of 0.15, 0.15 and 0.25 μg ml^{-1} in the regioisomers of **1**, **2** and **3** respectively. However, the *ortho*, *meta* and *para*

regioisomers of the methylephedrine gave a higher quantification level of 0.83, 1.03 and 0.30 μg ml^{-1} respectively. The difference between the compounds can be attributed to the difference in the UV absorbing functional groups. The limit of quantification when comparing **3** to that reported by Santali *et al*.[4] show a similar response. The paper gives a LOD of 0.09 μg ml^{-1} and a LOQ of 0.28 μg ml^{-1}. [4]

The robustness of the method was measured by monitoring the change in the relative retention time. The temperature was varied by 2ºC above and below the target temperature 30ºC. The RRT was calculated from the respective regioisomers of methylmethcathinone. The increase in temperature resulted in a small variation but this was not a significant change in the RRT which would inhibit analysis. The decrease in temperature gave a closer RRT to that of the expected temperature. Looking at Table 14 the data for the change in relative RRT for all three regioisomers can be seen the method gives a bigger increase in RRT when the temperature was raised. This would be because the viscosity of the mobile phase was changed allowing for the analyte to move easier through the column.

The mobile phase composition gave the biggest alteration to the RRT but these are not significant enough to stop analysis being performed. The changes in RRT for mobile phase composition was expected as the HILIC mode is very sensitive to the amount of water present in the mobile phase. But the largest change in RRT was 0.1 minutes with **4**-**6**.

The flow rate was altered by 0.1 mL min^{-1} and gave no variation in RRT showing that the variation in the flow rate will not interfere with the analysis.

Table 14 The robustness data for **1** - **6**.[a] Mobile phase composition is acetonitrile to ammonium formate 5 mM aqueous. [b] Relative retention time relates **1** to **4**, **2** to **5** and **3** to **6**. a=Red trace in figure 22. b=Green trace in figure 22. c=Blue trace in figure 22

	Mobile Phase Composition						Temperature						Flow rate					
	89:11[a]		90:10		91:9		28 °C		30 °C		32 °C		0.9 mL min^{-1}		1 mL min^{-1}		1.1 mL min^{-1}	
	t_R	RRT[b]	t_R	RRT	t_R	RRT	t_R	RRT	t_R	RRT	t_R	RRT	t_R	RRT	t_R	RRT	t_R	RRT
1[a]	6.49	1	6.60	1	7.50	1	6.49	1	6.60	1	7.50	1	7.37	1	6.60	1	6.06	1
4[a]	8.21	1.26	9.37	1.42	11.05	1.47	9.44	1.40	9.36	1.42	9.49	1.44	10.46	1.42	9.36	1.42	8.58	1.42
2[b]	6.68	1	6.86	1	7.89	1	6.98	1	6.86	1	6.84	1	7.64	1	6.86	1	6.28	1
5[b]	8.47	1.27	9.39	1.37	11.28	1.43	9.44	1.35	9.39	1.37	9.48	1.39	10.46	1.37	9.39	1.37	8.60	1.37
3[c]	6.89	1	7.2778	1	10.184	1	7.368	1	7.2778	1	6.574	1	8.07	1	7.28	1	6.63	1
6[c]	8.62	1.25	9.63	1.32	14.24	1.40	9.63	1.31	9.63	1.32	9.47	1.44	10.66	1.32	9.63	1.32	8.77	1.32

Looking at the accuracy experiment, all three regioisomers perform well with a recovery of 100% and a %RSD of no more than 1.5% in the *ortho*-regioisomer **4**. This is likely due to an inaccuracy in the balance as well as the slightly different weights used; the sample weight was 10.2 mg whereas the standard was 10.0 mg.

Table 15 The results from the recovery experiment on **3** using the mobile phase 5 mM aqueous ammonium formate - acetonitrile [10:90% v/v] on the ACE-SIL 5 (150 x 4.6 mm 5 µm) column.

Analyte	4-methylmethcathinone						
Replicate	Peak Area (Sample)			Peak Area (Standard)			Assay
(Sample)	Injection	Injection	Mean	Injection	Injection	Mean	
	80% (8.0 µg mL^{-1})						
1	545.36	544.02	544.69	549.7	547.9	548.8	99.25
2	546.97	545.19	546.08				99.50
	100% (10.0 µg mL^{-1})						
1	670.17	671.56	670.86	678.3	678.1	678.2	98.92
2	674.54	674.09	674.31				99.43
	120% (12.0 µg mL^{-1})						
1	813	813.20	813.10	815.5	817.2	816.35	99.60
2	813.42	813.30	813.36				99.63
						Mean	99.39
						SD	0.27
						%RSD	0.27

Table 16 The results of the recovery experiment for **6** using the mobile phase 5 mM aqueous ammonium formate - acetonitrile [10:90% v/v] on the ACE-SIL 5 (150 x 4.6 mm 5 µm) column.

Analyte	4-methylephedrine						
Replicate	Peak Area (Sample)			Peak Area (Standard)			
(Sample)	Injection 1	Injection 2	Mean	Injection 1	Injection 2	Mean	Assay %
			80% (16.0 µg mL-1)				
1	640.69	641.03	640.86	640.00	639.66	639.83	100.16
2	640.401	642.48	641.44				100.25
			100% (20.0 µg mL-1)				
1	785.83	785.65	785.74	784.48	780.54	782.51	100.41
2	783.92	783.96	783.94				100.18
			120% (24.0 µg mL-1)				
1	946.80	946.24	946.52	946.05	944.84	945.44	100.11
2	948.93	945.65	947.29				100.20
						Mean	100.22
						SD	0.10
						%RSD	0.10

Table 17 The results from the recovery experiment on **2** using the mobile phase 5 mM aqueous ammonium formate - acetonitrile [10:90% v/v] on the ACE-SIL 5 (150 x 4.6 mm 5 µm) column.

Analyte	3-methylmethcathinone						
Replicate	Peak Area (Sample)			Peak Area (Standard)			
(Sample)	Injection 1	Injection 2	Mean	Injection 1	Injection 2	Mean	Assay %
			80% (8.0 µg mL^{-1})				
1	241.38	241.49	241.43	241.21	241.27	241.24	100.08
2	241.81	241.72	241.77				100.22
			100% (10.0 µg mL^{-1})				
1	301.02	301.51	301.26	298.48	297.59	298.04	101.08
2	301.83	301.29	301.56				101.18
			120% (12.0 µg mL^{-1})				
1	353.15	352.15	352.65	348.52	348.72	348.62	101.16
2	353.58	354.09	353.84				101.50
						Mean	100.87
						SD	0.58
						%RSD	0.57

Table 18 The results of the recovery experiment for **5** using the mobile phase 5 mM aqueous ammonium formate - acetonitrile [10:90% v/v] on the ACE-SIL 5 (150 x 4.6 mm 5 µm) column.

Analyte	3-methylephedrine						
Replicate	Peak Area (Sample)			Peak Area (Standard)			
(Sample)	Injection 1	Injection 2	Mean	Injection 1	Injection 2	Mean	Assay %
	80% (16.0 µg mL^{-1})						
1	599.69	599.30	599.50	598.73	599.97	599.35	100.0
2	597.97	597.72	597.85				99.75
	100% (20.0 µg mL^{-1})						
1	755.35	752.88	754.12	755.74	754.68	755.21	99.86
2	756.67	756.77	756.72				100.2
	120% (24.0 µg mL^{-1})						
1	917.92	917.95	917.94	919.66	915.84	917.75	100.0
2	917.36	918.65	918.01				100.0
						Mean	99.98
						SD	0.16
						%RSD	0.16

Table 19 The results from the recovery experiment on **1** using the mobile phase 5 mM aqueous ammonium formate – acetonitrile [10:90% v/v] on the ACE-SIL 5 (150 x 4.6 mm 5 µm) column

Analyte	2-methylmethcathinone						
Replicate	Peak Area (Sample)			Peak Area (Standard)			
(Sample)	Injection 1	Injection 2	Mean	Injection 1	Injection 2	Mean	Assay %
	80% (8.0 µg mL^{-1})						
1	680.77	681.16	680.96	680.61	681.37	680.99	99.99
2	680.31	680.96	680.63				99.95
	100% (10.0 µg mL^{-1})						
1	846.40	846.87	846.64	846.79	846.97	846.879	99.97
2	846.22	846.22	846.22				99.92
	120% (12.0 µg mL^{-1})						
1	1014.31	1013.25	1013.78	1013.06	1012.25	1012.66	100.11
2	1013.15	1014.73	1013.94				100.13
						Mean	100.01
						SD	0.09
						%RSD	0.09

Table 20 The results of the recovery experiment for **4** using the mobile phase 5 mM aqueous ammonium formate - acetonitrile [10:90% v/v] on the ACE-SIL 5 (150 x 4.6 mm 5 µm) column

Analyte	2-methylephedrine						
Replicate	Peak Area (Sample)			Peak Area (Standard)			
(Sample)	Injection 1	Injection 2	Mean	Injection 1	Injection 2	Mean	Assay %
	80% (16.0 µg mL^{-1})						
1	241.38	241.488	241.43	235	235	235	102.74
2	241.49	241.72	241.61				102.81
	100% (20.0 µg mL^{-1})						
1	846.40	846.87	846.64	846.79	846.97	846.88	99.97
2	846.22	846.22	846.22				99.92
	120% (24.0 µg mL^{-1})						
1	1014.31	1013.25	1013.78	1013.06	1012.25	1012.66	100.11
2	1013.15	1014.73	1013.94				100.13
						Mean	100.95
						SD	1.42
						%RSD	1.40

Table 21 The results of the selectivity study comparing the compounds **1** – **6** to other compounds of similar composition. using the mobile phase 5 mM aqueous ammonium formate - acetonitrile [10:90% v/v] on the ACE-SIL 5 (150 x 4.6 mm 5 µm) column. [a] RRT is relative to **3**.

Compound	RT (minutes)	RRTa (minutes)
1	6.62	0.93
2	6.72	0.94
3	7.12	1
4	9.4	1.32
5	9.39	1.32
6	9.09	1.28
7	5.76	0.81
8	8.33	1.17
9	9.09	1.28
10	9.09	1.28

Table 21 shows the results of the selectivity study. This shows that the method can separate compounds **1**-**8**, however, it is unable to separate compounds **9**, **10** and **4**-**6**. This is likely due to the similarities these three compounds have;

Figure 39 shows the structure for these compounds.

The reason that we see this separation pattern is due to the compounds having different steric effects from groups attached to key functional groups allowing the hydrogen bonding to take place. In the case of **10**, the lack of a methyl group has little effect on the t_R, which remains the same as **4**-**6**. However, **8** lacks a methyl group on the nitrogen and its t_R is greater than that seen in **10** and **1**-**3**. This would indicate that the carbonyl maybe limiting the hydrogen bonding taking place. The co-elution of **7** and **9** with **4**-**6** show that their stronger attraction to the aqueous layer is facilitated by the amine and the alcohol groups.

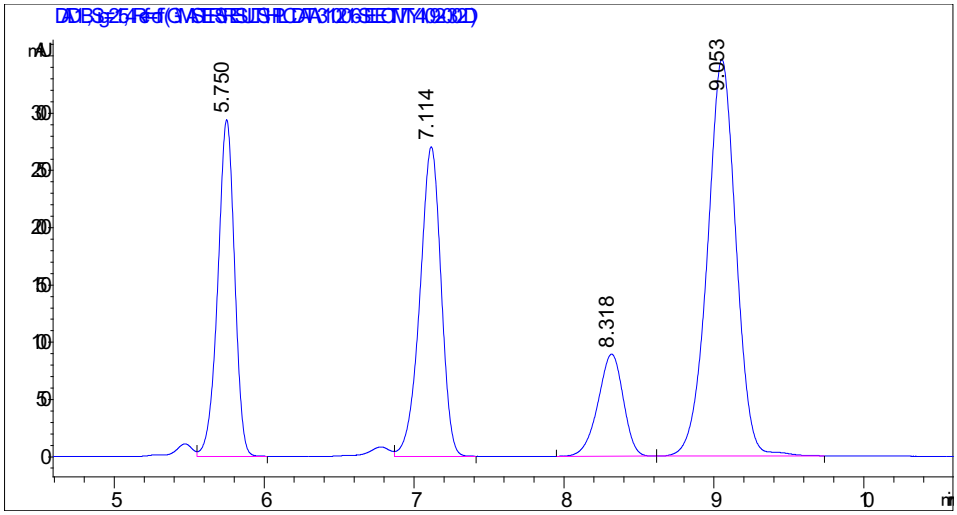

Figure 40 The chromatogram of the selectivity study using a mobile phase of 5 mM aqueous ammonium formate - acetonitrile [10:90% v/v] on the ACE-SIL 5 (150 x 4.6 mm 5 µm) column.

9. Conclusion

The synthesis of the methylephedrine *via* a reduction of the carbonyl on the methylmethcathinone using sodium borohydride has been demonstrated. The resulting three regioisomers of the 2, 3 and 4-methylmethcathinone reductions (i.e. the methylephedrines) were characterised using a variety of methods such as NMR and mass spectrometry. NMR spectra showed that there were structural similarities between compound **1**-**3** and **4**-**6**, however, there were clear and distinct differences which were used for the positive identification of the compounds. Most notably these were the addition of two proton environments at 6.1 ppm and 3.3 ppm corresponding to OH and CH respectively. Mass spectrometry (GC-MS in EI mode) showed the same results with key components of the spectra remaining the same.

The HPLC-HILIC separation of the methylmethcathinone and methylephedrine was only successful in terms of separating the two compounds, but was unable to separate the regioisomers, which was the aim of this project. However, the separation of the two groups was in fact a good starting point for which future candidates can build up from. As this method will allow a fast analysis of the compounds in under 10 minutes. The method reported has an excellent reproducibility %RSD < 1.5 and a linear co-efficient of > 0.9998. The accuracy of the method to its target concentration 20 μg mL^{-1} or 10 μg mL^{-1} for methylephedrine and methylmethcathinone respectively is no more than 2% in the 80%, 100% and 120% targets.

10. Future Work

This preliminary work indicates the potential for the separation of regioisomeric cathinones (in this case methylmethcathinones) from both themselves and their reduced methylephedrine derivatives (a primary phase 1 metabolite). Access to the other primary matabolites of mephedrone only became available at the end of the study and initial work (Table 21, Figure 33) indicates a HILIC approach to their separation is feasible. The separation of compounds (**6** & **10**) is not clear, however, it may be possible to differentiate these two analytes through either further method development (for example: optimising the mobile phase-stationary phase combination to achieve separation) or a more sensitive (or selective) detection techniques (for example: high resolution mass spectrometry). The former would involve optimisation/screening of the HILIC method with a variety of buffers, organic modifiers and stationary phases to improve the separation of the regioisomers. This could potentially be a more polar column such as an amino type stationary phase. The latter approach would be the combination of HILIC with mass spectrometry (as is applied in bioanalytical methods utilising LC-HRMS) to separate these primary metabolites from 4-methylmethcathinone. This resulting method would then need to be validated to be run to determine the LOD and LOQ and then test it against real case samples – however before this could be used routinely a bioanalytical/extraction from the biological medium (either blood or urine) would need to be developed/optimised. The additional benefit of this approach would give a secondary confirmation source, the mass spectra, other than the retention time. It would also allow the differentiation of the metabolites by mass. The author appreciates that this study only represents a preliminary investigation into this area, however, should the method be further developed – the potential and value of this

study towards the detection of either existing regioisomeric cathinones or new cathione derivatives as they become available on the illicit drug market is clearly apparent.

11. References

1. J. D. Power, P. McGlynn, K. Clarke, S. D. McDermott, P. Kavanagh and J. O'Brien, *Forensic science international*, 2011, **212**, 6-12.
2. Ó. J. Pozo, M. Ibáñez, J. V. Sancho, Lahoz-Beneytez, J. Esther, R. d. l. T. Papaseit, F. Hernández and M. Farré, *Drug Metab. Dispos.*, 2015, **43**, 248-257.
3. B. Buszewski and S. Noga, *Analytical and bioanalytical chemistry*, 2012, **402**, 231-247.
4. E. Y. Santali, A.-K. Cadogan, N. N. Daeidb, K. A. Savageb and O. B. Sutcliffe, *J. Pharm. Biomed. Anal.*, 2011, **56**, 246–255.
5. R. Mullins, A Change To The Misuse Of Drugs Act 1971 : Control Of Mephedrone And Other Cathinone Derivatives, https://www.gov.uk/government/statistics/tables-for-drug-misuse-findings-from-the-2012-to-2013-csew, (accessed June 2016).
6. H. M. Government, Misuse of Drugs Act 1971, https://www.legislation.gov.uk/ukpga/1971/38/contents, (accessed 17/09/2018, 2018).
7. P. Reuter and B. Pardo, *Addiction*, 2016, **112**, 25–31.
8. Home Office, Factsheet: Overview of the Misuse of Drugs Act 1971, https://www.gov.uk/government/uploads/system/uploads/attachment_data/file/455578/20150821_-_Fact_sheet_-_MDA.pdf, (accessed December 2016).
9. Home Office, Circular 028/2015: Misuse of Drugs Act 1971 (Temporary Class Drug) (No. 3) Order 2015 - Publications - GOV.UK, https://www.gov.uk/government/publications/circular-0282015-misuse-of-drugs-act-1971-temporary-class-drug-no-3-order-2015, (accessed December 2016).
10. C. Mayorga, I. Doña, E. Perez-Inestrosa, T. D. Fernández and M. J. Torres, *International Journal of Molecular Sciences*, 2017, **18**, 1222.
11. Home Office, Psychoactive Substances Act 2016, http://www.legislation.gov.uk/ukpga/2016/2/contents/enacted, (accessed June 2016).
12. F. Schifano, A. Albanese, S. Fergus, J. L. Stair, P. Deluca, O. Corazza, Z. Davey, J. Corkery, H. Siemann, N. Scherbaum, M. Farre, M. Torrens, Z. Demetrovics and A. H. Ghodse, *Psychopharmacology*, 2011, **214**, 593-602.
13. C. Davidson and F. Schifano, *Prog. Neuro-Psychopharmacol. Biol. Psychiatry*, 2016, **64**, 267–274.
14. The centre for social justice, Drugs in prisons, http://www.centreforsocialjustice.org.uk/library/drugs-in-prison, (accessed January 2017).
15. D. Wingfield, Drug Misuse: Findings from the 2015/16 Crime Survey for England and Wales, https://www.gov.uk/government/uploads/system/uploads/attachment_data/file/564760/drug-misuse-1516.pdf, (accessed January 2017).
16. J. R. H. Archer, P. I. Dargan, S. Hudson, S. Davies, M. Puchnarewicz, A. T. Kicman, J. Ramsey, F. Measham, M. Wood, A. Johnston and D. M. Wood, *J. of Substance Use*, 2014, **19**, 103-107.
17. J. Smith, O. Sutcliffe and C. Banks, *Analyst*, 2015, **140**, 4932-4948.

18. Advisory Council on the Misuse of Drugs Consideration of the cathinones, https://www.gov.uk/government/publications/acmd-report-on-the-consideration-of-the-cathinones, (accessed December 2016).
19. C. L. German, A. E. Fleckenstein and G. R. Hanson, *Life sciences*, 2014, **97**, 2-8.
20. A. M. Weinstein, P. Rosca, L. Fattore and E. D. London, *Frontiers in Psychiatry*, 2017, **8**, 156.
21. H. Torrance and G. Cooper, *Forensic Sci. Int.*, 2010, **202**, 62–63.
22. Home Office, Tables for 'Drug misuse: findings from the 2012 to 2013 CSEW', https://www.gov.uk/government/statistics/tables-for-drug-misuse-findings-from-the-2012-to-2013-csew, (accessed December 2016).
23. O. o. N. Statistics, User guide to drug misuse statistics, https://www.gov.uk/government/publications/user-guide-to-drug-misuse-declared-findings-from-the-crime-survey-for-england-and-wales, (accessed 16/07/2018, 2018).
24. O. I. G. Khreit, M. Grant, T. Zhang, C. Henderson, D. Watson and O. B. Sutcliffe, *J. Pharm. Biomed. Anal.*, 2013, **72**, 177-185.
25. M. Concheiro, M. Castaneto, R. Kronstrand and M. A. Huestis *J. Chromatogr. A*, 2015, **1397**, 32–42.
26. N. Satthaphut, O. B. Sutcliffe and I. Oswaldiain, *zkri*, 2014, **229**, 101.
27. Europol-EMCDDA, Joint Report on a new psychoactive substance: 4-methylmethcathinone (mephedrone), http://www.emcdda.europa.eu/html.cfm/index132196EN.html, (accessed December 2016).
28. S. Gibbons and M. Zloh, *Bioorg. Med. Chem. Lett.*, 2010, **20**, 4135–4139.
29. P. Jankovics, A. Váradi, L. Tölgyesi, S. Lohner, J. Németh-Palotás and H. Kőszegi-Szalai, *Forensic Sci. Int.*, 2011, **210**, 213–220.
30. J. R. Peters, R. Keasling, S. D. Brown and B. B. Pond, *J. Anal. Toxicol.*, 2016, **40**, 718-725.
31. R. W. H. Perera, I. Abraham, S. Gupta, P. Kowalska, D. Lightsey, C. Marathaki, N. S. Singh and W. J. Lough, *J. Chromatogr. A*, 2012, **1269**, 189-197.
32. S. Mohr, M. Taschwer and M. G. Schmid, *Chirality*, 2012, **24**, 486-492.
33. M. Taschwer, J. Grascher and M. G. Schmid, *Forensic Sci. Int.*, 2017, **270**, 232-240.
34. J. Le, Drug Metabolism, http://www.msdmanuals.com/en-gb/professional/clinical-pharmacology/pharmacokinetics/drug-metabolism, (accessed April 2016).
35. A. Green, M. King, S. Shortall and K. Fone, *Br. J. Pharmacol.*, 2016, **171**, 2251-2268.
36. T. Scientific, HILIC Separations, http://apps.thermoscientific.com/media/cmd/flipbooks/TG-21003-HILIC-TG21003-EN_flipbook/index.html, (accessed December 2016).
37. A. J. Alpert, *J Chromatogr*, 1990, **499**, 177-196.
38. A. J. Alpert, *Chromatography Today*, 2015, **8**, 4-7.
39. Y. Guo and S. Gaiki, *J. Chromatogr. A*, 2005, **1074**, 71-80.
40. X. Li, C. E. Uboh, L. R. Soma, Y. Liu, F. Guan, C. R. Aurand, D. S. Bell, Y. You, J. Chen and G. A. Maylin, *Rapid Commun. Mass Spectrom.*, 2014, **28**, 217-229.

41. G. Frison, S. Frasson, F. Zancanaro, G. Tedeschi and L. Zamengo, *Forensic Sci. Int.*, 2016, **265**, 131-137.
42. United Nations Office on Drugs and Crime, Recommended methods for the Identification and Analysis of Synthetic Cathinones in Seized Materials, https://www.unodc.org/unodc/en/scientists/recommended-methods-for-the-identification-and-analysis-of-synthetic-cathinones-in-seized-materials.html, (accessed December 2016).
43. United Nations international drug control programme, Rapid Testing Methods of drugs of abuse, https://www.unodc.org/pdf/publications/st-nar-13-rev1.pdf, (accessed December 2016).
44. K. E. Toole, S. Fu, R. G. Shimmon and N. Kraymen, *Microgram Journal*, 2012, **9**, 27-32.
45. K. Himanshu, Master in Science in Pharmaceutical Analysis, University of Strathclyde, 2013.
46. Interntional Conference for Harmonisation, Validation of Analytical Procedures: Text and Methodology, http://www.ich.org/products/guidelines/quality/quality-single/article/validation-of-analytical-procedures-text-and-methodology.html, (accessed January 2017).
47. L. Bijlsma, J. V. Sancho, F. Hernandez and W. M. Niessen, *Journal Mass Spectrom*, 2011, **46**, 865-875.
48. K.-A. Kovar and M. Laudszun, *Journal*, 1989.
49. G. N. Wogan, S. Paglialunga, M. C. Archer and S. R. Tannenbaum, *Cancer Res.*, 1975, **35**, 1981.
50. C. L. O'Neal, D. J. Crouch and A. A. Fatah, *Forensic Sci. Int.*, 2000, **109**, 189-201.
51. N. Nic Daeid, K. A. Savage, D. Ramsay, C. Holland and O. B. Sutcliffe, *Sci. Justice*, 2013, **54**, 22-31.
52. M. K. Nahoko Uchiyama, Ruri Kikura-Hanajiri, Yukihiro Goda, *Forensic Sci. Int.*, 2013, **227**, 21–32.
53. S. Analytical, Improving HPLC Performance: Relationship between particle size, column efficiency and column pressure, http://www.sigmaaldrich.com/analytical-chromatography/hplc/columns/ascentis-express/technical-resources.html, (accessed December 2017).
54. Center for Drug Evaluation and Research, Reviewer Guidance Validation of Chromatographic Methods, http://www.fda.gov/downloads/drugs/guidancecomplianceregulatoryinformation/guidances/ucm134409.pdf, (accessed January 2017).
55. I. Linhart, M. Himl, M. Židková, M. Balíková, E. Lhotková and T. Páleníček, *Toxicol. Lett.*, 2016, **240**, 114–121.